Determination of the Influence of Microwaves to the Hard Rock Characteristics and to the Cutting Process

To the Faculty of Geosciences, Geo-Engineering and Mining

of the Technische Universität Bergakademie Freiberg

Approved

MASTER THESIS

To attain the degree of Master of mining

Submitted by

Leonid Chebenko

Born on the 23rd of February 1992 in Ukraine

Reviewers:

Prof. Dr. Carsten Drebenstedt, TU Bergakademie Freiberg

Prof. Dr. Illya Gumennik, National mining university

Declaration of Authorship I hereby certify that this thesis has been composed by me and is based on my own work, unless stated otherwise. No other person's work has been used without due acknowledgement in this thesis. All references and verbatim extracts have been quoted, and all sources of information, including graphs and data sets, have been specifically acknowledged.

Date: Signature:

Acknowledgement

I specially would like to thank my parents who gave me pure love and support me during all my live.

I would like to express my very great appreciation to my supervisor Prof. Dr. Carsten Drebenstedt for opportunity to do this research, for all his guidance, useful critiques and suggestions.

I would like to thank Dr. Andrii Cherep for opportunity to study in this program, providing repeated assistance throughout the period of study.

I would cordially thank Dr. Philipp Hartlieb who helps me with microwave test in Leoben in the beginning of study, for valuable advice and support in the side measurement.

My grateful thanks are also extended to the Mr. Bruno Grafe for his help in 3D modeling, calculation cutting process, doing laboratory test, and assistance in keeping my progress on schedule.

I would like to offer my special thanks to Dr. Taras Shepel who helped me perform statistical analyses in research, modeling in Solidworks, valuable suggestions during all investigation.

Special thanks to my friends, Natalia Rodionova for her helps in English and Ievgen Liubymtsev for him enthusiastic encouragement, care and support during writing this work.

Table of contents

CHAPTER ONE

1.1   Introduction

The most energy-intensive and expensive process during extraction and mineral processing is their destruction. For example, in iron ore mining and processing plant in Russia this process results in 70% of total energy consumption (~ 30 kWh / t of ore) [1]. Among all the destruction processes such as drilling, blasting and, crushing, grinding is the most energy-intensive one (-26 kWh / ton of ore) [1]. As far asmining industry in the US is concerned, share of crushing and grinding amounts to 29.3 billion KWh per year, which is 45% of the total consumption of electricity by the US mining industry [2]. That explains why in recent years there is such a great practical interest to optimize the usage of energy during excavation and to develop   new ways of emolliating ores and minerals, new energy-saving technologies of grinding ore. Traditionally, consuming energy can be expressed as the concept of specific energy, i.e. the amount of energy required to remove a unit volume of rock (J/m^3).

Generally there are two possibilities of inputting energy to the rock for excavation: one is by blasting, second is by mechanical excavation. Figure 1-1 illustrates these methods where energy input is related against time. [3]
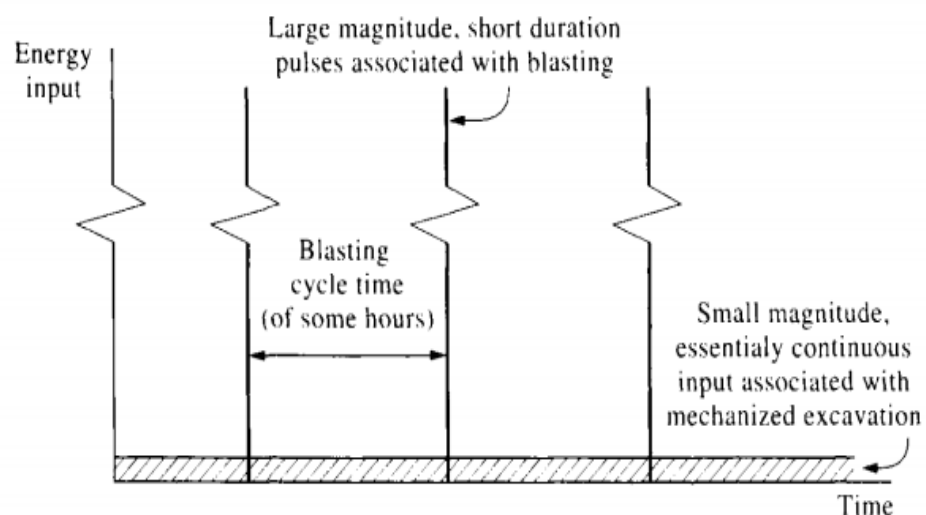

Figure 1 - 1: Energy input rates for blasting and mechanical excavation

The energy is either input in large amount during a short time, or in smaller quantities continuously. The conclusion from this is the following: excavation of minerals has to use a cyclical method with blasting or a continuous method by machine.

A roadheader, continuous miner or tunneling boring machine (TBM) is commonly used for rock breakage applications in underground . Nevertheless, in some cases blasting method cannot be applied for all parts of mining technology due to negative impact in the vicinity of settlements and urban areas. Another advantage of roadheaders and TBM excavation compared to blast is production of a smooth and accurate tunnel with a low rock reinforcement cost of the operation. Therefore, roadheader has a problem with penetration rate when working in abrasive rock, wjich leads to a high consumption cutting tool. Other affecting parameters that have impact on this machine are described in Chapter 1. Originally, roadheaders found application in soft to medium strength lithologies like coal, potash and salt [4].

As per the previous research [5] and [6] fracture of rock can be achieved by applications of different types of energy such as, electrical (sputter-ion, electrostrictive and piezoelectric), magnetic (magnetostrictive), electromagnetic (laser), sound (impact plastic, ultrasonic), beam (electrons, protons and plasma) and thermal.

Electromagnetic energy is the most promising one out of the studied forms of energy, in terms of ability to influence the physical and mechanical properties of minerals and rock. The advantages of softening in the microwave electromagnetic fields are the following:

- conversion of microwave energy into thermal energy, within penetration depth, depending on the frequency of the electromagnetic field;
- high heating temperature, allowing to provide high-speed softening commensurate with the speed of mechanical loading [7].

The basic concept of microwave heating is that microwaves cause molecular motion by immigration of ionic species and/or rotation of dipolar species. Microwave heating a material depends to a great extent on its 'dissipation' factor, which is the ratio of dielectric loss or 'loss' factor to dielectric constant of the material to retard microwave energy as it passes through; the loss factor is a measure of the ability of the material to

dissipate the energy. In other words, 'loss' factor represents the amount of input microwave energy that is lost in the material by being dissipated as heat. Therefore, a material with high loss factor is easily heated by microwave energy [8].

The research is needed to find new methods of hard rocks destruction, which will allow better and more efficient production of fracture and dressing of the rocks. The advantage of microwave processing of rocks before grinding may be increasing the selectivity of the disclosure of rocks and cuttability of the rock [9].

1.2 Framework of Thesis

The topic of thesis proposed by Professor Carsten Drebenstedt is "**Determination of the Influence of Microwaves to the Hard Rock Characteristics and to the Cutting Process".** The project was organized in cooperation between two universities with Montanuniversität (Leoben, Austria) and TU Bergakademie (Freiberg, Germany). The main aim of the work was to increase the knowledge of the behavior of microwave treatment of hard rock for subsequent cutting process. Due to the temperature gradient in the samples induced by the microwave irradiation, a significant damage is indicated by a reduction of the sound velocity and finally, the formation of cracks occurs. [10] Evolving a cutting machine (roadheaders, continuous miner and TBM) that could be used in hard rock, based on a combination of conventional and alternative rock, breaking methods would be a major advantage for the application in new and future mining and tunneling operations [11]. The thesis comprises of 6 chapters which are as follows:

Chapter 1 describes present technologies of the excavation, which are used for hard rock. Advantages and disadvantages of mining underground machines and the parameters that affect to the performance of these machines.

Chapter 2 is devoted to the history of microwaves application in mining. Describes the method of microwaves treatment for softening rock, as well as physical properties of microwaves propagation and their nature. It introduces characteristics which have affected rock: rocks permittivity, temperature gradient, and others.

Chapter 3 is devoted to theory of cutting test, the main parameters which impact to specific energy consumption and wear of cutting tool.

Chapter 4 presents preparing samples for the tests. There is describes implementation of large-scale microwave facility and cutting machine as well as parameters which were used during the test. In this chapter described the methods of processing the data and calculations.

Chapter 5 is dedicated to the result. There are presents bar charts with relationship of microwave energy to cutting force as well as wear rate, and mesh size analyses.

Chapter 6 is final chapter, where the conclusion and future work recommendations.

1.3   Excavation in Hard Rock

Excavation technology for hard rock cutting has essential prospects for selective mining, continuity and automation of operations over drill-blast out system that suffers from cyclic nature of its operations. Nowadays, available continuous rock cutting technology is, however, restricted generally to the excavation of relatively `weak rocks` due to its capital and running costs and the physical size problems associated with mechanical design [12].

In the past few years, the development of tunnel machines has reached a level, at which they are used to an increasing extent, not only in soft rock but also in hard rock. Performance of these machines depends on the following parameters that can be divided into three groups: mechanical, geological-geotechnical and technical-operational which are described in Table 1.

Table 1 - 1: Summary of parameters affecting roadheader performance (after Fowell, R. 1982)

Summary of Parameters Affecting Roadheader Performance

Mechanical Parameters	Machine Type (Crawler Mounted, Shielded, Twin Boom, etc.) Machine Weight and Dimensions Boom Force Capacities (Shearing, Lifting, and Lowering) Cutterhead Type (Transverse, Axial) Cutterhead Power and RPM, Lacing Design Bit Type and Dimensions, Metallurgical Properties of Tip
Geological–geotechnical parameters	*Rock Mass Properties* RQD Bedding, foliation, and fault zones Joint sets (orientation, spacing, filling, etc.) Hydrogeology (water table/water ingress) Adverse geology (squeezing, swelling, and blocky grounds) *Physical and Mechanical (Intact Rock) Properties* Cuttability (cutter forces, SE, and optimum cutting geometry: linear cutting tests) Strength (UCS, BTS, elasticity modulus, cohesion, etc.) Texture and abrasivity (mineral/quartz content and grain size, microfractures, grain interlocking, etc.) Others (brittleness, water content, swelling, etc.)
Operational parameters	*Technical Parameters* Tunnel shape and dimensions Inclinations, crosscuts *Mining Parameters* Support (bolting, shotcrete, steel sets, etc.) Muck haulage (conveyor, locomotive, LHD, etc.) Utility lines (power, water, and air supply) and surveying Ground treatment (drainage, grouting, and freezing) Labor availability and quality

Limits of excavation process, hard and abrasive rock that belong to the geological characteristics lead to a decrease in performance of the machine and in turn increase the wear resistance of cutting tools, which play important role in pick consumption

[pick/solid m^3]. Roadheaders, TBM and another rock-cutting machine generally use two types of cutting tools, namely indenters and drag picks. The difference between these tools is the way in which they penetrate rock massive. Indenters are often used in full-face scale operations of TBMs and capable excavate rock with uniaxial compressive strength (UCS) up to 350 MPa, mainly close to civil tunneling projects. Roadheaders find implementation in partial face and step operation because of the flexibility and mobilization of the equipment and can excavate rock with their drug bits with uniaxial compressive strength of 80MPa while heavy duty roadheaders can cut rocks up to 100MPa. Figure 1 presents ratio between CERCHAR abrasivity index and Uniaxial Compressive strength.

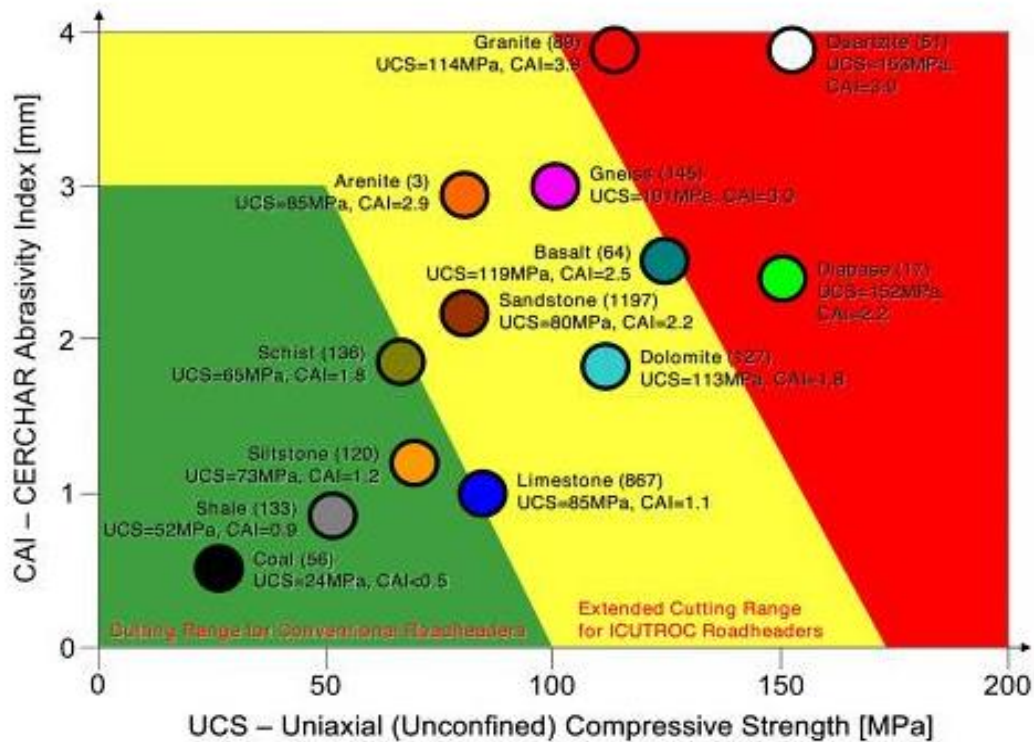**Figure 1 - 2: The relationship between CAI and UCS (Figure of Sandvik Mining and Construction)**

Another important role that affects the cutting process is a rock mass classification. Previous research (Bilgin 1996) shows that performance of roadheader can be predicted with RQD and compressive strength of rock for instantaneous cutting rate. Figure2 presents ratio between RQD and instantaneous cutting rate. [13]
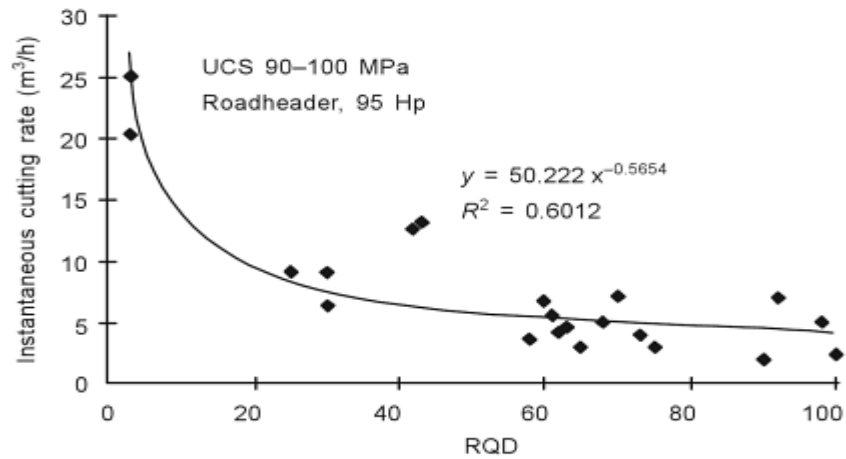
Figure 1 - 3: Instantaneous cutting rate versus RQD (after Bilgin et. al 1996)

Geotechnical system RMR was developed by Bieniawski, 1973 for estimation load, rock condition and tunnel support. Recently, classification of RMR has been applied to excavation coal and hard rock. Publications of Johnson 1991, Sanbak 1985 show correlation between RMR and cutting performance of a heavyweight TMB (operational catting rate and bit consumption) [m^3h]. It was observed, that RMR value, RQD value, existence of discontinuities (joints spacing, cracks net) can be used for prediction of rock cuttability and estimation performance of excavation machines.

CHAPTER TWO

2.1 History of Microwave Irradiation in Mining Industry

Mining Institute A.A .Skochinskiy developed several types of the destruction of boulder and investigated in an industrial environment using high-frequency electromagnetic energy. These studies identified two main ways that allow crushing all the boulders of hard rock: 1) high-frequency thermal breakdown method, and 2) nonuniform dielectric heating method. Implementation of particular method is primarily determined by electro physical parameters of the rock.

In terms of electrical properties (conductivity, dielectric permittivity, dielectric loss tangent), minerals are divided into two main classes: semiconducting minerals (iron ore, rich ores of nonferrous metals, etc.) and rocks dielectrics (granite, sandstone, limestone, gneiss, poor ores of nonferrous metals). The properties of rocks changing under the influence of electric and thermal fields.

The first method of high frequency destruction is used for crushing semiconducting rocks, the second one applied - for the rock-dielectrics. The essence of the method of high frequency thermal crushing is as follows: electrical energy feeding from the high-frequency generator to cable by direct contact between two rod electrodes to rock. High frequency breakdown occurs between electrodes that form a conductive channel. The high-power energy can direct to this channel from high-frequency generator or from capacitor in the form of pulse discharge. In this case, thermoelastic stresses appear in the rock leading to failure. Thermal breakdown and destruction of boulder ferruginous quartzite with weighing up to 40t had been carried out in laboratory and industrial applications with a power range of 30-100 KWt and frequency of 70-300 KHz when the distance between the contacts was 2m. Time of breakdown was 10-60 sec.

Industrial high-frequency machines have been created and tested to estimate effectiveness of the contact method; self-propelled mounting IGD, movable installation LOR -60 and to units for underground condition named LPR-40. Performance of movable installation LOR -60 and self-propelled mounting in YGOK were equal to 12-15 m^3/h. Mean time to failure 1t of ore on transportable part was 45-60 seconds at a cost of electricity of 1-3 kWh.

The high-contact method was tested in underground Gubkin mine and on the open pit of Krivoy Rog. Energy consumption of LPR-40 was determined at the current frequency of 250 kHz and 40 kW of the destruction boulder with volume of 0.35 - 0.50 m^3 which was 3-5 kWh/t. The performance of LPR-40 in Gubkin underground mines was 10-12 m^3/h.

The key point of the destruction rocks-dielectrics is that under the electrodes nonuniform heating of rock occurs, which leads to destructive thermal stress.

The facility "Eletra" was tested on non-metallic production in 1965, which was investigated by Skochinskiy University. The most extensive studies have been conducted on the destruction of boulders. Research of destruction boulders was carried out on "Rovnoe", "Akademicheskoe", "Sokolovskoe", "Golovinskom", quarry's.
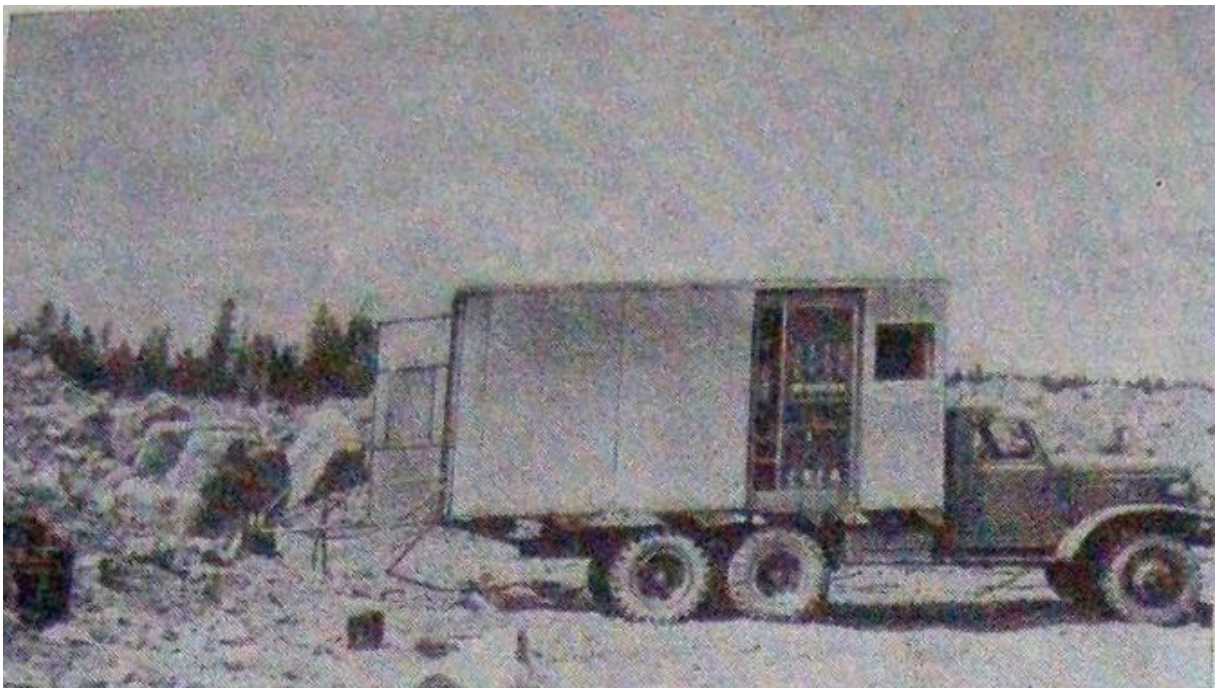
Figure 2 - 1: High-frequency facility "Electra" in the open-pit Rovnoe (YGDK 1969)

Studies in the open pit Sokolov, Golovin, "Rovnoe" proved the effectiveness of the high- frequency fragmentation of boulders. The performance of 15m3/h has been achieved during boulders fragmentation of volume up to 7,5m3 on open pit.

2.1 Microwave Irradiation

The Scottish physicist James Maxwell expressed the hypothesis of the existence of electromagnetic waves in 1864. Microwaves are a type of electromagnetic

radiation. The length of waves ranging from 1mm with frequency 300 GHz until 1m with frequency 300 MHz receptively (Fig.2-2). The length and frequency of wave obey the equation 2-1 [14].

$$c= \lambda * f \qquad \qquad 2\text{-}1$$

where: c – speed of light (299 792 458 m/s);

λ – length of wave (m);

f - frequency (Hz)
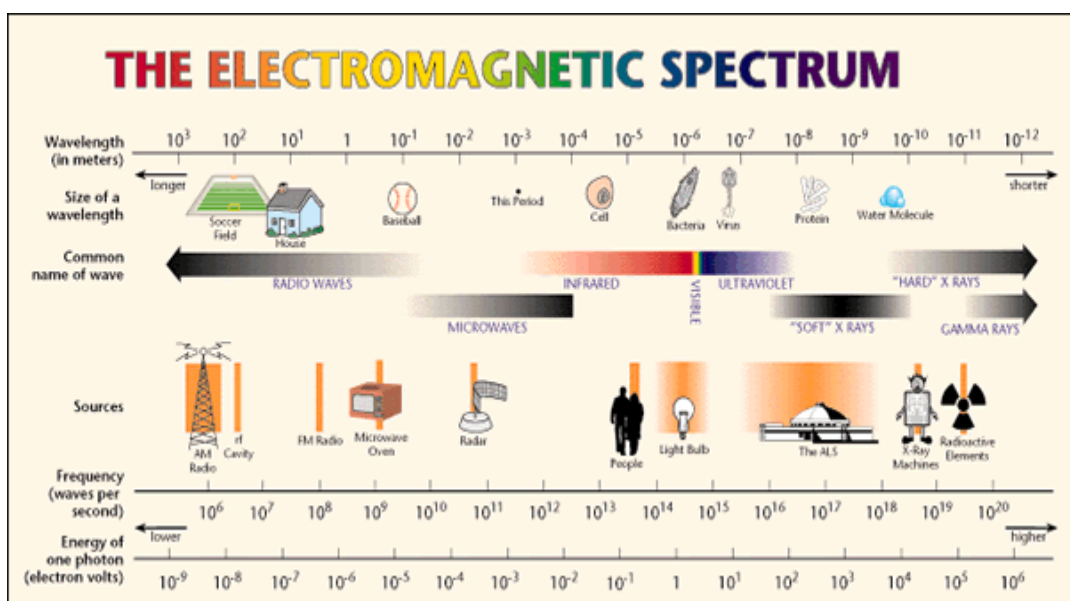
Figure 2 - 2: Electromagnetic spectrum [15]

Microwaves occupy a medium position between radio and infrared radiation. This intermediate position of microwaves has an effect on their properties. Microwave radiation has properties as radio waves and light waves. For example, this radiation spreads in a straight line as light and can overlap almost all solid objects. The electromagnetic waves oscillations in electric and magnetic fields which are perpendicular to each other and to the direction of wave (Fig. 2-2).

Figure 2 - 3: Electromagnetic waves (Scott, 2006)

According to the theory of Maxwell's time-varying electric field, the magnetic field is generated. Electromagnetic waves propagate through space in the form of transverse waves at the speed of light.
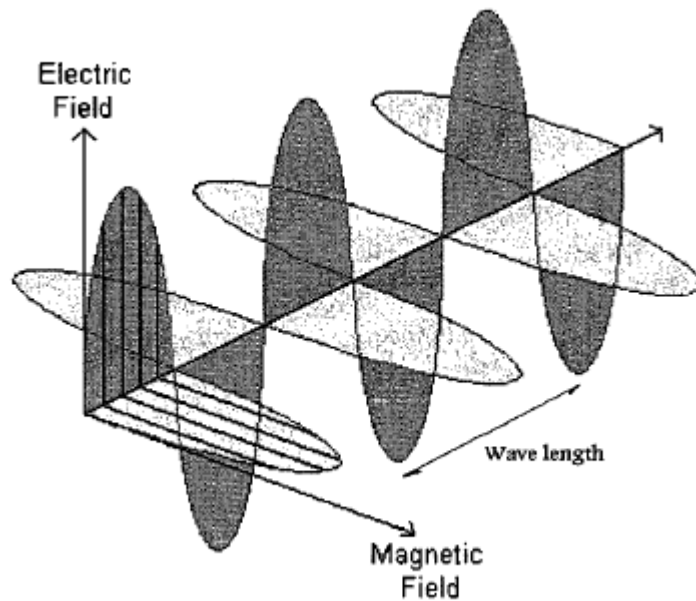
All materials react differently to microwave radiation. It is well known, that all materials in nature are divided into three major groups by conductivity:

- conductors (usually metals) with the resistance $10^{-6} - 10^{-3}$ Ohm*cm;
- insulators (air, gases, plastic) with resistance $10^{9} - 10^{20}$ Ohm*cm;
- absorbers, material which can absorb a part of microwave energy.

The material that can absorb microwave energy is called dielectrics. The absorption of microwave radiation in a rock depends on complex permittivity ε and can be defined as:

$$\varepsilon = \varepsilon' - j\varepsilon'' \qquad \qquad 2\text{-}2$$

Where: ε - complex relative permeability measured in farad per meter (f/m).

ε' - the real part of the dielectric permeability associated with polarization under the influence of the applied field;

ε'' - the imaginary part, related to the finite conductivity of the dielectric [16].

When the dielectric constant changes with constant permeability in a vacuum is called the complex relative permittivity.

$$k = k' - k'' \qquad 2-3$$

Where k – is complex relative permeability; k' - is the dielectric constant; k'' - imaginary loss factor.

The tan δ – is tangent loss factor, can be expressed as:

$$\tan \delta = \frac{k''}{k'} \qquad 2-4$$

The absorbed energy propagates within the rock with losses. The materials classifies into two groups:

1. Low loss – tan δ <<1;
2. High loss – tan δ >>1.

The emitted microwave energy penetrates into material until a certain depth. The effective penetration depth can be defined when power attenuated to a 1/e the power at the surface. The penetration depth in dielectric materials expressed as:

$$D_p = \frac{\lambda e^{1/2}}{2\pi k''} \qquad 2-5$$

Equation 2 -5 use for low loss dielectric materials (k''/k'<<1), and

$$D_p = \frac{\lambda}{2\pi k''^{\frac{1}{2}}} \qquad 2-6$$

Equation 2-6 use for high-loss dielectric materials (k''/k'>>1) [17]. Where λ - is the appropriate electromagnetic wavelength in meters.

As a consequence internal compressive and shear stresses are expected to build up causing cracks, which are responsible for reduction of rock strength consequently leading to a reduction of mechanical energy required for fragmentation of the rock mass or even to a fragmentation solely due to the microwave absorption. [18]

CHAPTER THREE

3.1 Basics of cutting process

The main idea of this study is to minimize specific energy consumption. In order to identifyi changes of rocks properties and to estimate specific energy as a consequence of microwave irradiation, a mechanical cutting test was used. Several properties should be taken into account in the breakage process (in this case cutting process) of the rock and selection of the optimal equipment and tools. The main ones are the characteristics of intact rock and they should include the following characteristics:

- Compressive strength
- Tensile strength;
- Hardness and abrasiveness of the rock
- Index of the dynamic and contact plasticity
- Rock texture and shape. [19] [20]

3.2 Cutting Force and Theories

Breaking rock can be achieved by implementation of three kinds of tools: indenters, drug bits, and roller cutter. Difference between indenters and drug bits is that indenters breaking a rock by applying a force which is normal to surface. Generally drug tools are applied on partial-face machine to mine a medium-strength rock. The choice of one of the types of cutting tool depends on the mentioned characteristics above as well as machine type and size. Selecting a proper tool and strategy can have a main role in the cutting efficiency, excavation cost and machine performance.

Usually, drug bits or radial cutting tools are used in soft rock not very abrasive rock, conical picks used in medium-strength and more abrasive rock (<100MPa), and for strength and abrasive rock applying a disc cutter or strawberry cutters. It is also very important to take into account the cutting forces that have impact on the bit that determines the usability and applicability in a particular field of implementation. [19] [21]

The effect of drag bits is to cleave rock chips from the surface. A share force is acting to the rock by bit, but the rock breaks due the growth of tensile crack. In other words, cutting process take place when tensile strength of rock is exceeded. [22] [23]

There are many methods and theories to estimate the cutting force such as rock cutting test or using an analytical and empirical formula.

One of the cutting theory was borrowed from metal machining cutting theory development by Merchant's (1944). Shuttleworth adopted theory to discontinuous regime (brittle, discrete chipping) and proposed the equations for normal and cutting forces:

$$Fc = \frac{\sigma_s \cdot d \cdot w \cdot \cos(\phi_f - \alpha)}{sin\phi \cdot \cos(\phi + \phi_f - \alpha)} \qquad (3-1),$$

$$Fn = Fc \cdot \tan(\phi_f - \alpha) \qquad (3-2),$$

Where Fc – is the cutting force, Fn – is the normal force, σ_s – is the shear strength, d – is the depth of cut, w – is the tool width, ϕ – is the angle of internal friction of the rock, ϕ_f - is the friction angle between the wedge and the rock, α - the tool rake angle.

Although, the model is limited, the following characteristics were ascribed:

51 Indicates a liner extension cutting force with increase of cutting depth;

52 Shows decrease of forces with increasing rake angle.

53 Describes linearly increasing bits forces with rock strength.

Another cutting theory was proposed by Evans (1962) for soft and medium strength rock. Firstly, the model was for a symmetrical wedge which is not suitable in practice

$$Fc = \frac{2 \cdot T_0 \cdot d \cdot sin\theta}{1 - sin\theta} \qquad (3-3)$$

Where T_0 - is the rock tensile strength, θ - is the half-angle of the wedge

But it was adopted to asymmetrical geometry of drug bit.

$$Fc = \frac{2 \cdot T_0 \cdot d \cdot sin\frac{1}{2}(\frac{\pi}{2} - \alpha)}{1 - sin\frac{1}{2}(\frac{\pi}{2} - \alpha)} \qquad (3-4)$$

In this model Evans argued the following:

2.1 The force R acts to rock under friction angle δ in plane A-C

2.2 The total force of tensile stress T acting to center of curve C-D

2.3 The penetration of drug smaller than layer h_i

The R force acting near the C point and can be written as the following expression:

$$R = \frac{\sigma_t \cdot h_i \cdot w}{2 \cdot \sin(\beta) \cdot \cos(\alpha + \beta + \delta)} \qquad (3-5)$$

Where σ_t – tensile strength, h_i – thickness of layer cut, β - the shear angle, δ - soil external angle of friction.

From (3-5) the β – shear angle can be find use the formula

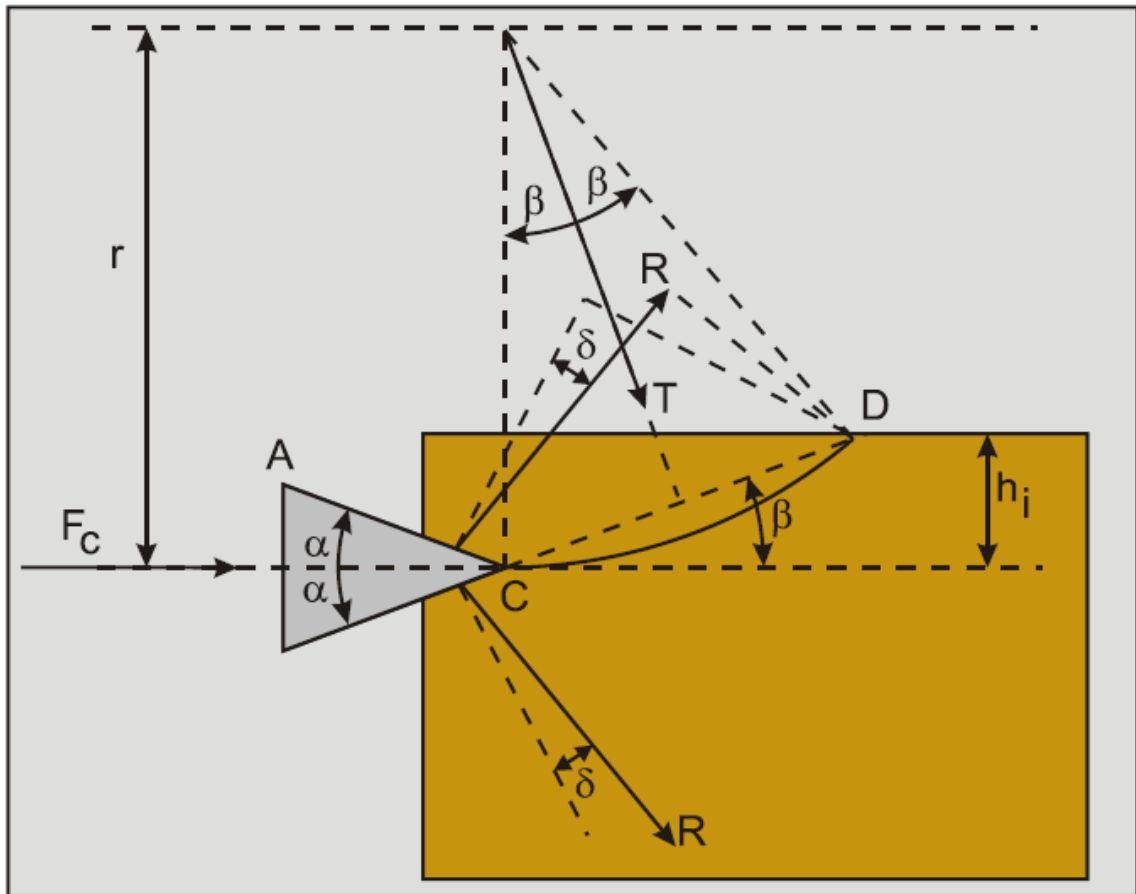$$\beta = \frac{\pi}{4} - \frac{\alpha + \delta}{2} \qquad (3-6)$$

Figure 2 - 1: Evans' model (after Evans)

In practice it was obtained that this formula gives an accuracy variations of cutting force. Nishmatsu's theory (1972) was an alternative and involved a Coulumb-Mohr failure criterion in the line of plane to equation and summarized cutting forces of drug bits

$$Fc = \frac{2 \cdot \sigma_s \cdot d \cdot w \cdot cos\phi}{(n+1) \cdot [1 - sin(\phi - \alpha + \phi_f)]} \qquad (3-6)$$

Where   n   –   stress   distribution   factor   and   can   be   obtained   as

$$n = 12 - \frac{\alpha}{2} \qquad (3-7)$$

This model gives a right result for a brittle shear rock. According to this theory, a cutting force acting through shear stress. Nishmatsu argued the following:

    2.1 The rock cutting is brittle, lack any plastic deformation.

    2.2 The cutting process is under plain stress contribution

    2.3 The failure is according a liner Mohr envelope

    2.4 The cutting speed has no influence on cutting process.

       The difference between theory of Nishimatsu and Merchant that Nishimatsu assumed that breakage of rock occurs due the impact of shear failure while Merchants argued that this happens due to plastic deformation in steel and clay cutting. [24]

3.3   Influence Geometry of Pick

       Influence of tool geometry elements on the power and energy performance of cutting rocks is looked into by a number of studies. The effect on cutting force parameters is consistently taken into consideration: (fig. 3-2)

    - cutting angle Ɣ and a rake angle α;

    - clearance angle β;
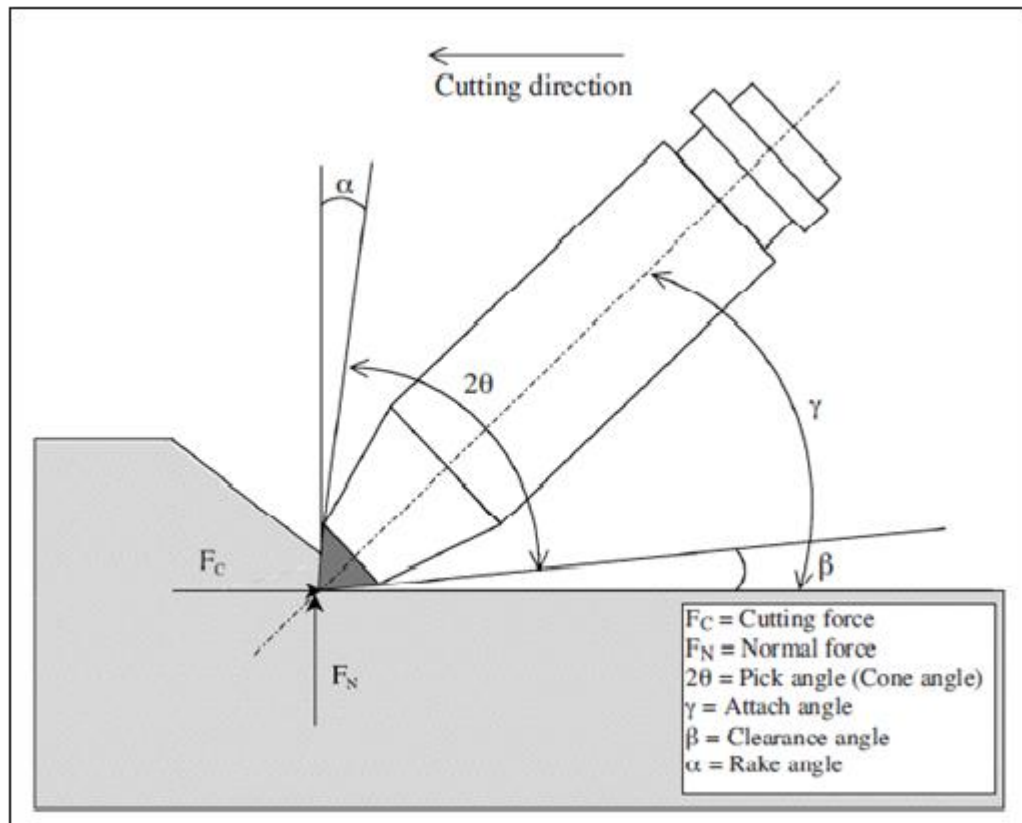
    - the width of the cutting edge (width of pick)

Figure 3 - 2: Geometry of pick penetration (after Goktan 2005)

Attach angle or cutting angle Y. Many research and industrial experiments show that this element of the tool geometry is one of the most important. Therefore, correct choice of the angle of cutting has significant impact on significance in the design of wedge.

V.N. Getopanov has investigated the influence of the cutting angle on the power characteristics of the process and established that with increasing of the cutting angle the cutting increases continuously, especially intensively when $Y > 90^0$ i.e. at negative rake angles.

This is due to the fact, that the picks with $Y > 90^0$ (attach angle) has height of the side cutting edges with the rock, as measured along the axis of the tool, reaches the depth of cut, and as a result, base of area compacted core and their volume significantly increases. Therefore, there is a decline of the conditions of output particles (chip formation) from the undercutting zone and additional overgrinding.

The core interest to us constitutes dependence of the following two factors:

- In most cases cutting force increases proportionally to the cutting angle;

- When increasing cutting angle by more than 90^0 ,i.e. at negative rake angles, growth cutting forces become more intensive.

21

Clearance angle β. This angle is essential to the formation of the forces acting on the pick. Observations show that layer of rock located in undercutting area is elastically deforming. As a result, a contact area between the back face of pick and rock is formed.

Reduction of the volume of these areas and reduction of the cutting forces and feeding force can be achieved by increasing the clearance angle. Excessive increasing of the clearance angle β at the same cutting angle α leads to a significant decrease of the strength of the tool because of necessity to reduce the wedge angle.

Taking this into consideration, it is important to take into account specific energy consumption and the strength of the tool during selection of clearance angle β.

V.N. Getopanov established reduction of the cutting force with increasing of clearance angle β from 2.5 to 7.5^0 during cutting of shale.

According to Belorussov, cutting force is reduced by increasing the clearance angle up to $8{-}10^0$ regardless of the thickness of chips (plot. 3-1). Further increasing of the clearance angle has no effect on cutting force.
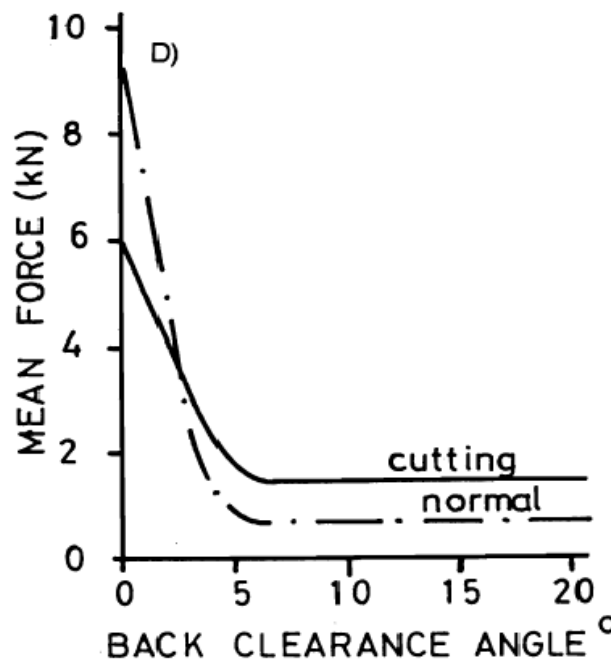

Figure 3 - 3: Effect of clearance angle to cutting force (SME Handbook 2009)

Rake angle α. Special attention should be paid to the rake angle. Increasing the rake angle over the optimum leads to higher energy consumption and also to increasing of a wear of pick. Heavy wear leads to greater contact with the clearence surface of the tool

22

with working area of rock and, as a result, to a significant increase in the resulting cutting force. Nevetheless, increasing rake angle from small to higher amount induces a degression contact area in tool and surface, and leads to reduction of total cutting force. The negative rake angle also has a negative impact, the contact area increases and causes a higher chip formation, as a result force also increases. [25]
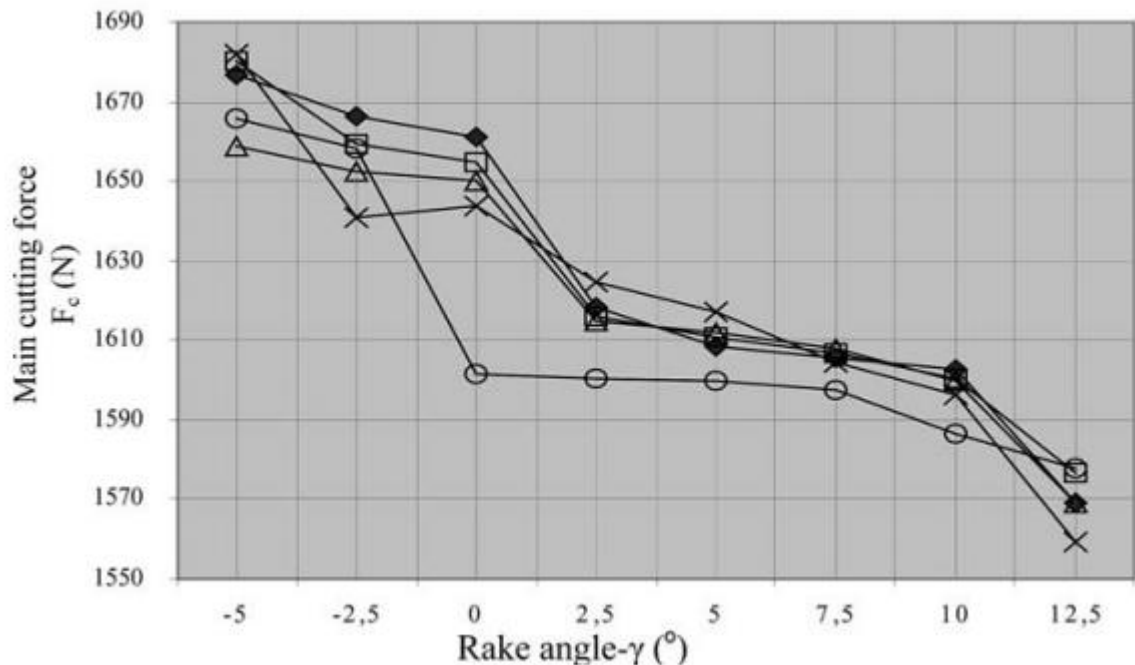

Figure 3 - 4: Relation between cutting force and rake angle

The gragh 3-2 shows how cutting force increases against a rake angle. The cutting forces decrease when the rake angle changes from mines value to a positive direction. The cutting forces are much or less stable from a $0^0 - 7,5^0$.

Depth and Width of Cut. Spacing and depth between cuts (chip thickness) greatly affect the cutting force and specific energy consumption during cutting process. The dependence of the cutting force on cutting spacing (s) is examined in a number of studies. All of them indicate that with increasing distance between cuts, cutting force (Fc) increases which leads to an increasing specific energy. Moreover cutting force (Fc) increases only to a certain limit, after which further increase of the cutting spacing (s) has no effect on the cutting force (Fc). [20] There is an optimal distance between the cuts in the rock that is consistent with the minimum specific energy consumption. The optimum spacing is multiple of cutting depth. This peculiarity is well known as ratio between spacing and depth (s/d ratio). This value can range from 1.5 – 3 (s/d) for point

attack pick, depending on the type of rock. The relation between spacing and depth is shown in Fig. 3 – 2.

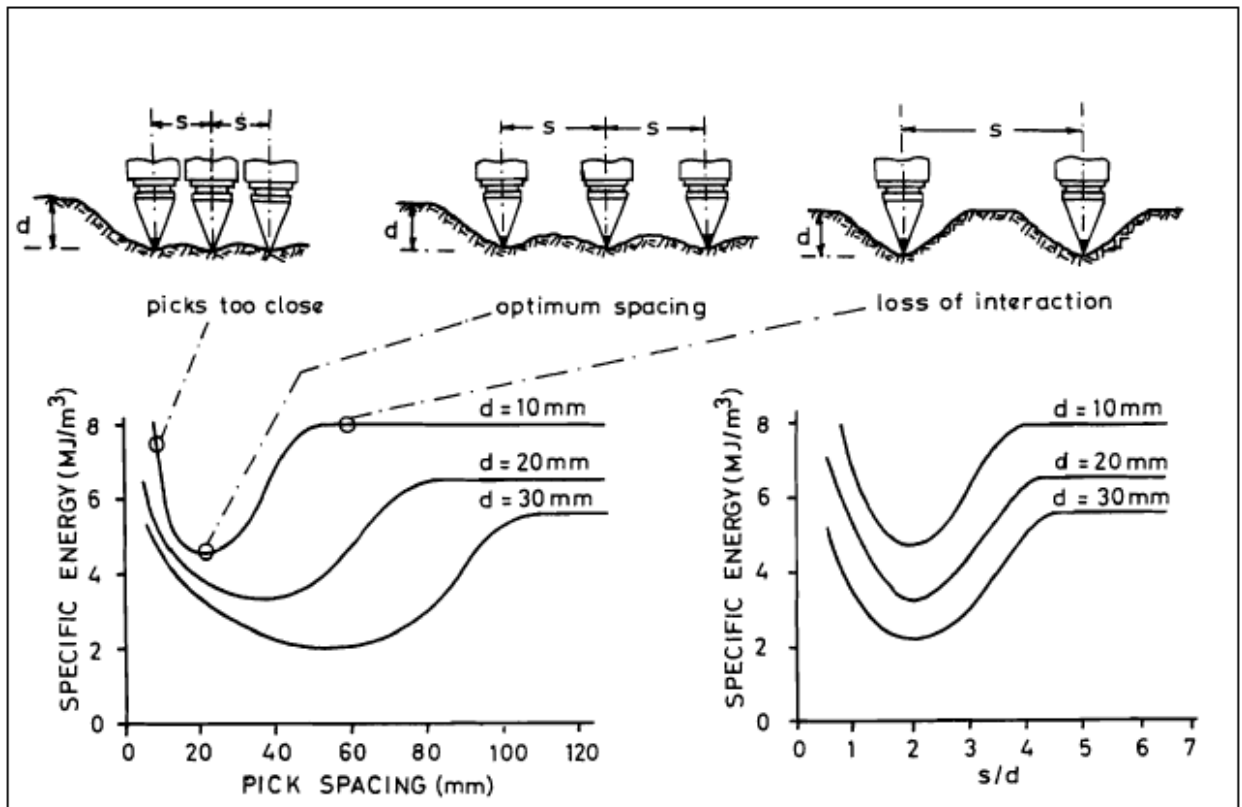**Figure 3 - 5: Relation between spacing and depth s/d (SME Handbook 2009)**

When the spacing between cuts is too small the cutting process is not efficient due to over crushing the rock. When the spacing is too big, the cutting is also not efficient, because radial cracks cannot reach each other as shown in Fig. 3 -6.
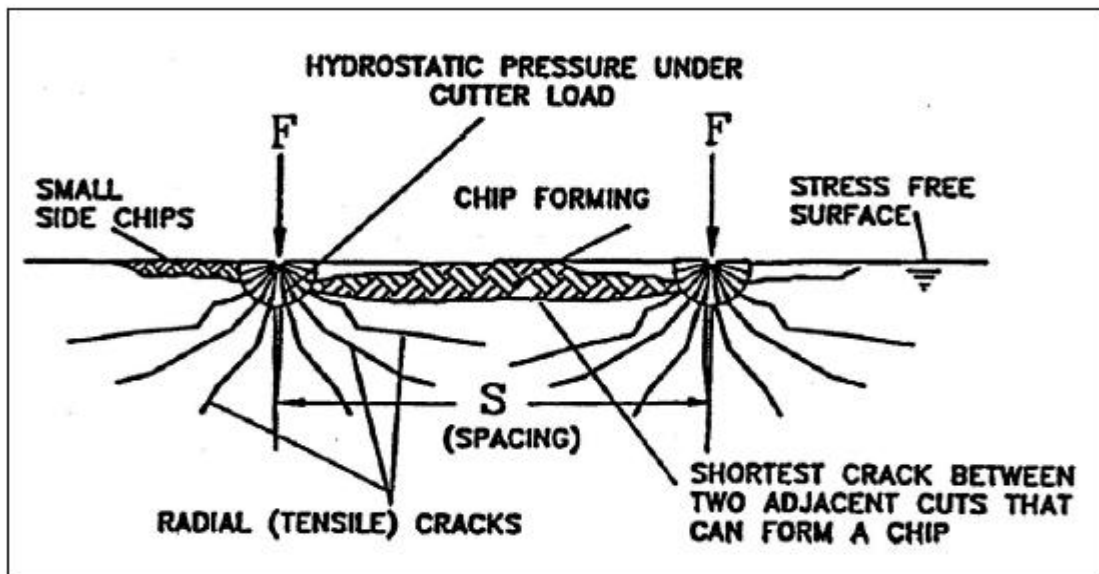

Figure 3 - 6: Forming the radial cracks during cutting process (SME Handbook 2009)

3.4 Specific energy

To determine the specific energy in laboratory rest the following formula was used:

$$SE = \frac{Mean\ cutting\ force(kN)}{Yield\ (m^3)} = \frac{MJ}{m^3} \quad 3-8$$

$$Yield = \frac{area\ of\ cutting\ surface(m^2) * m(for\ 1m\ of\ cutting\ length(m^2)}{m(for\ 1\ m\ of\ cuttig\ length)} = \frac{m^3}{m}$$

Since SI units are used in the literature , it's necessary to convert formula to another unit.

$$SE = \frac{Mean\ cutting\ force(kN)}{3,6 * Yield\ (m^3)} = \frac{KW * h}{m^3} \quad 3-9$$

3.5 Wearing of pick

Prediction of performance excavation is a main concern of many studies and dependence on the bit consumption. Wear of cutting toll in this work is not the main study, however, it should be included in the data processing. The wearing of tool depends on such factors as:

- characteristics of material that wearing the cutting tool;
- characteristics of the cutting tool;
- conditions of the environment where process carried out.

Hardness and Abrasivity. Since in this work a hard rock (in this case granite) is used , it is an important factor that has effect to wear is an abrasion. It was the main subject of many studies, particularly how an abrasivity affect the wear [26] [27]. They pointed out that an increase in the index of abrasiveness rock cutter wear increases respectively. One of the components the investigated rock is silica (SiO_2), which is the main accessary to wear the pick. Another important factor relating to wear is hardness of rock that has the same influence as abrasion. The rate of wear increases with the index of hardness. According to Protodiyakonov scale (rock hardness scale from 1 to 20), the granite has a hardness of 15. Since the impact of microwave assists in breaking the rock, as it is expected to reduce hardness of granite and abrasivity as well as, a result consuming a wear rate should be reduced. There are different methods to calculate the wear rate. Most of them used the unit [bits/m^3]. Since in this research not many bits were used, it was decided to make a measurement of wear with another unit

[weight/length]. To calculate a wear rate, picks were weighed beforehand and after cutting test, then difference was divided by the length of cut (formula 3 - 10).

$$W = \frac{m_2 - m_1}{l_c}, \left[\frac{g}{m}\right] \qquad 3 - 10$$

Where m_1 – mass of pick before cutting test (gram); m_2 – mass of pick after cutting test; l_c – length of cut (m).

Cutting speed and force. Influence of cutting speed to wear rate shows that with increasing cutting speed the wear of tool also increases. At high cutting speeds wear is mainly caused by high temperature. Since in this research its application was relatively small and constant cutting speed (0,1m/s) influence on the wear rate could not be determined. The cutting force is a significant factor to affect of wear rate. The resulting force can be divided into three components: cutting force Fc, side force Fs and normal force Fn. The cutting force acts in the direction of cutting, while the normal force acts perpendicular to cutting. These two forces have a main impact to wear, because the value of side force is usually smaller than others. To calculate the resultant force the following formula was used:

$$\vec{F_r} = \vec{F_c} + \vec{F_s} + \vec{F_n} \qquad 3 - 10$$

To wear development also affects ratio Fn/Fc [28]. When cutting tool becomes blunt, this ratio increases by several times.

CHAPTER FOUR

4. Experimental Apparatus and Procedure

4.1 Technical Parameters of Microwave Machine

The large scale microwave ring consists of two parts: 1 – microwave generator which supplies energy and 2- safety cavity for a safe conduct of experiments (Fig. 5-1).

Figure 3 - 1: The microwave facility (Magnetron and control unit on right side and safety cavity – left side)

This microwave generator was created by Mügge Company. The magnetron has a 2450 MHz frequency and 30 Kw maximum output power. Automatic tuner provides reduction of the possible reflections, as well as excellent relationship between samples and microwaves. The operator can control magnetron by using electronic unit, set the output power and time of operation. In addition operator can record essential parameters as reflected and forward power, actual frequency and phase of the waves.

The microwave facility completed with safety mechanisms. One of them is photo diode located near the magnetron which prevents lightning and electric arcs. The system turns off automatically when it detects an arc and lightning. Another mechanism is a circulator which deflects the reflected microwaves into the load water. This protects a magnetron from high reflected power. The waveguide has a permeable window

through which the waves pass but prevents travel dust through the waveguide (Fig. 4-2).
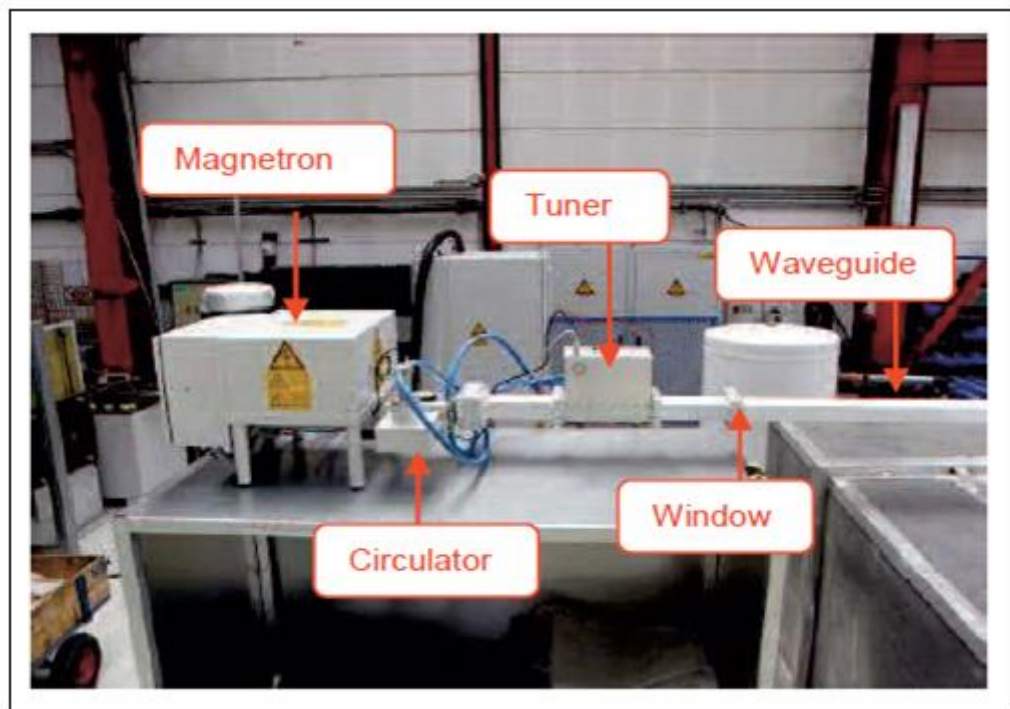
Figure 4 - 2: Safety mechanism of microwave testing rig

In the cavity the waveguide located directly above the samples, therefore supplied energy is directed precisely to the sample. The waveguide has a size of 32*64 mm^2. Also there is a sample tray inside cavity (Fig. 4-3).
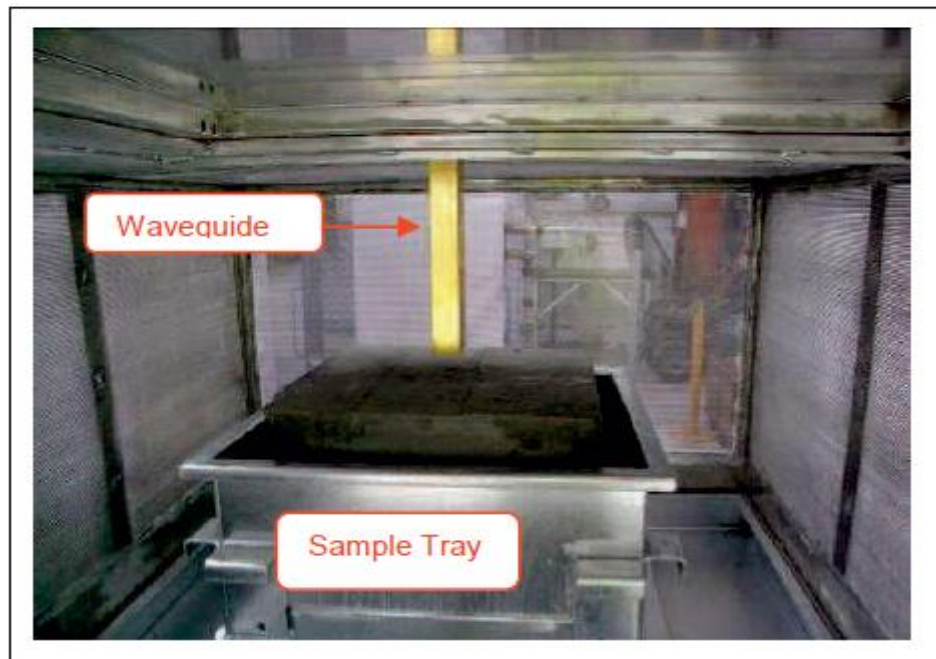
Figure 4 - 3: Inside view of cavity

It allows to dispose rock samples with size 50x50x30 (w*i*h). The tray can be moved along the x and y axis (through the length and breadth) inside the cavity with the help of two wheels which are located outside the cavity (Fig 4-4).
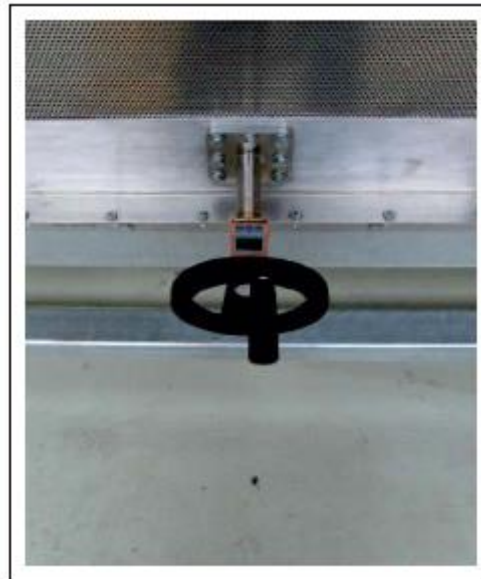
Figure 4 - 4: One of the two wheel for movement the tray samples

This enables to conduct the experiments more accurately. The cavity has door locks in case of unauthorized opening of the door during an experiments. On the top of cavity an irradiation sensor is located which reacts to radiation leakage (Fig. 4-5).

Figure 4 - 5: Irradiation sensor and an automatic door lock

4.2 Methods of Microwave Irradiation

The experiment was performed with treatment samples positioned at one spot. Two samples of granite were treated with different time intervals 30 and 45 seconds respectively. The third sample was treated for 30 seconds as the first one but the distance between the radiated spot has been reduced and due to the technical problems with facility only the half of the block was radiated. The size of the radiated spots approximately coincides with the dimensions of the waveguide (32 *64mm^2). The distance between radiated spots in 1 and 2 samples is 10 cm and 7.5 cm in the third. This method was chosen considering the fact that it was possible to calculate the amount of output power more accurately. The parameters of the experiment are shown in Table 6-1.

4.3 Calculation of Input Energy After Microwave Treatment of Samples

All the necessary test data was stored in file type ASCII, that could be usable in MS Excel for calculations. The file contains the following data:

- Time: time in seconds from the start of the program;
- No: number of measurement;
- F_MHz: frequency in MHz;
- Mag: magnitude of measured reflection coefficient;
- Phase: Phase of measured reflection coefficient;
- Pi_W: Incident power in watts;
- Pr_W: Reflected power in watts;
- Temp_C: Internal temperature of tuner in Celsius;
- Err: An internal error code;
- St1_mm: Position of the tuner stub1 in the waveguide;
- St2_mm: Position of the tuner stub2 in the waveguide;
- St3_mm: Position of the tuner stub3 in the waveguide.

To calculate the utilized power the following formula was used:

$$P_u = P_i - P_r \ [kW] \qquad\qquad 5-1$$

Where P$_u$ – absorbed power in kW; P$_i$ – power of incoming waves in Kw; P$_r$ – power of reflected waves in kW. The total energy can be calculated as:

$$E_t = P_u * t \ \ [kWt * h] \qquad\qquad 5-2$$

Where t – irradiation time in hour.

4.4 Metal Case for Radiated Blocks

After the microwave test the blocks were damaged. Cracks can be observed not only from the top surface where there was radiation, but also from the sides (Fig 4-6).

Figure 4 - 6: Block #2, radiated time 45 sec, side cracks

For this reason, there was a probability that during the cutting test, large pieces could fall off from the sample or even split the block in half that could lead to inaccurate results. To avoid this, special reinforced concrete case with metal rods of 10 mm thickness has been designed.

First, on the perimeter of the block has been welded metal construction from an armature (Fig. 4-7). The detailed sketch of case is located in Annex 2.
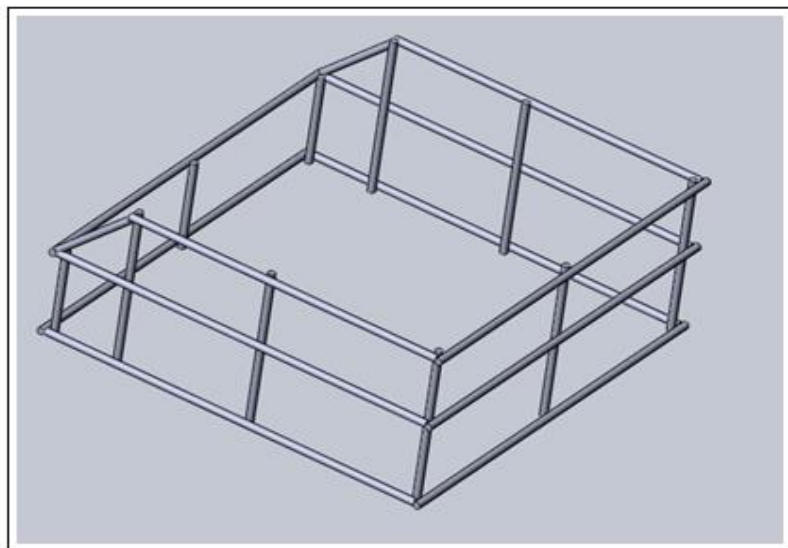

Figure 4 - 7: Metal case for damage blocks

Blocks #2 and #3 were filled with concrete thickness of 5 cm from each side. Dimensions of the case have been chosen taking into account the limits of the cutting machine (1000*600*600mm). On the front side of the concrete block, height of the wall was made lower than the height of the block (30 cm) for more convenient conducting of the cutting experiment (Fig. 5-8).
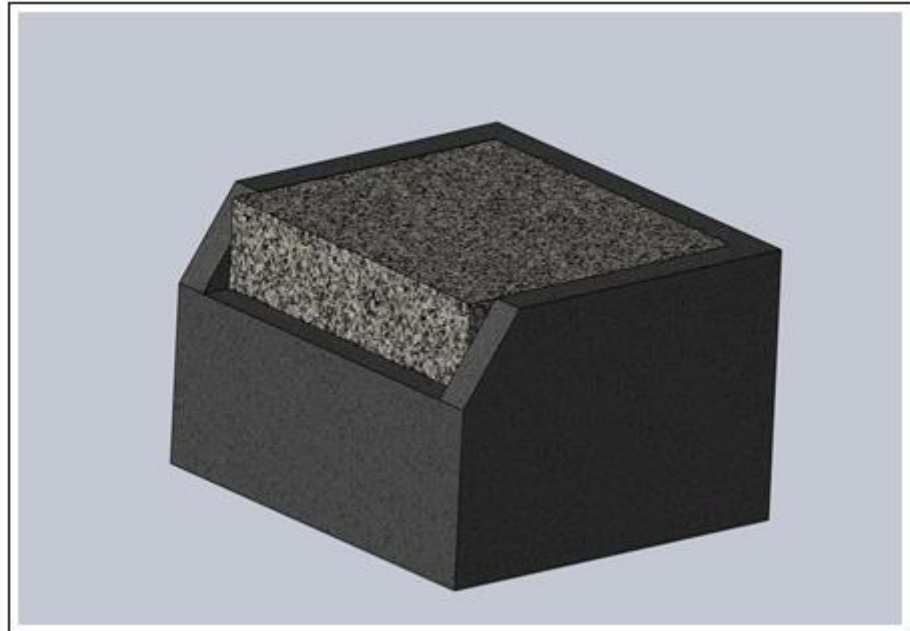
Figure 4 - 8: Block inside the concrete case with metal rods

Sand, cement and water were used to manufacture the concreate case. Ratio sand to cement was 3:1,1 kg of cement has been used to 3 kg of sand.

Two forms of concreate were molded for the uniaxial compressing strength. According to building regulations, brand strength of the concrete comes in 28 days after filling in normal conditions. In this case, these standards have been met.

4.5 Large Scale Cutting Rig

To evaluate damage from the effects of microwaves to rock, the large scale cutting ring was used. To perform cutting test, a special machine HXS is 1000-50 was applied. (fig. 5-1). The machine was developed by the company ASW GmbH Naumburg in 2008 specifically for cutting tests of various kinds of investigation. The machine is based on a CNC milling machines, but is largely modified to meet the requirements of cutting rocks.
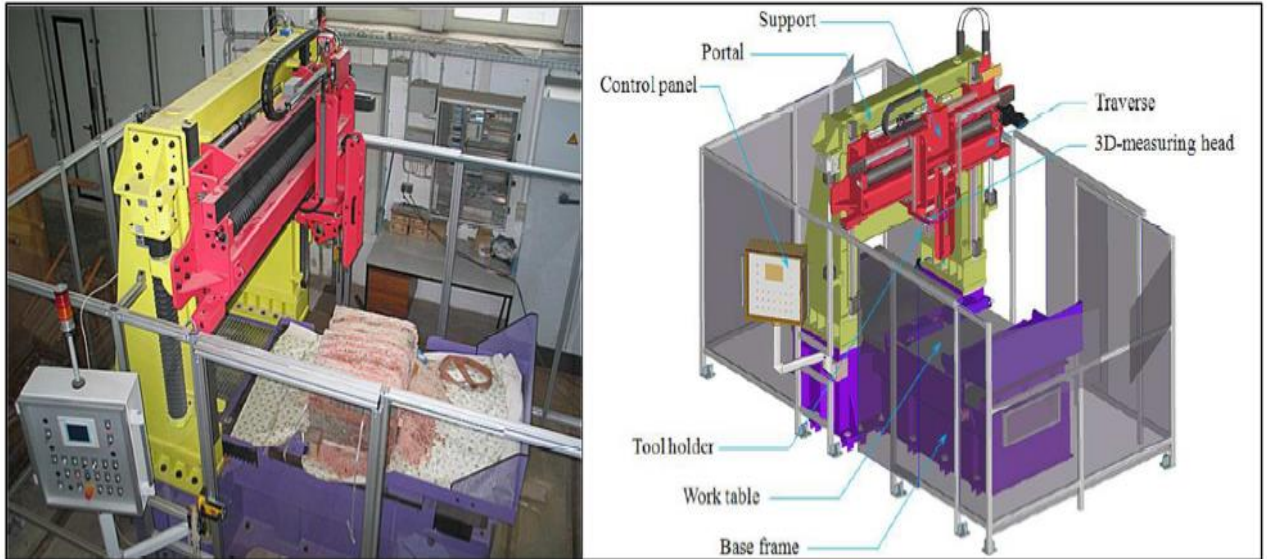
Figure 4 - 9: Photo (left) and scheme (right) of the large scale cutting machine [29]

The cutting head can be moved along two axes y and z, transverse and normal respectively. The average speed of this machine is up 1,75 m/s. Detection of the cutting force carried out by means sensors located in the head of the machine (fig. 4-2)
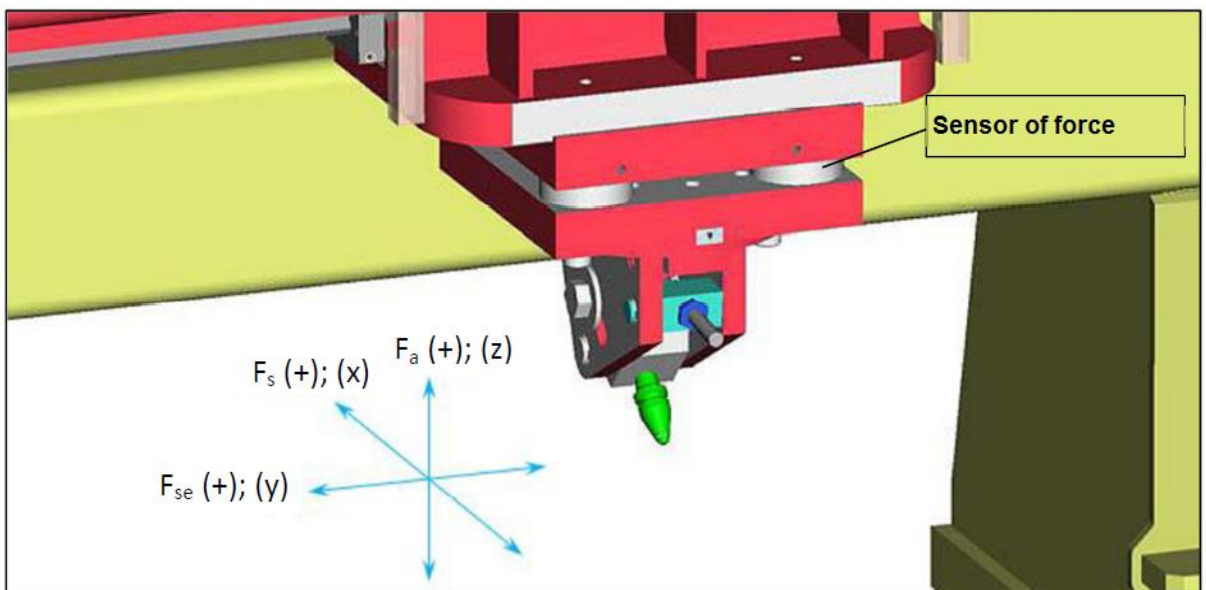
Figure 4 - 10: Definition of force components, axes position and sensors on the cutting head on the special planer HSX 1000-50 [29]

To determine the volume of cut rock, the laser measuring was used which located additionally on the cutting head. After each cut layer the surface was scanned to calculate the cut-out volume.

Further technical data of cutting rig is given in Annex I. The acquisition of the data values was performed via a computer the type DEWE 5000 (Fig. 4-11). The computer converts the signals received from the force measuring sensor located in the head machine with 16-bit digital converter with a digitalization frequency of 1000 kHz. The storage and analysis of measured values is carried out via the software DEWESoft.

Figure 4 - 11: Measuring computer DEWE 5000 for data acquisition and program package for DEWESoft

There are not only the force components added but also the bit position in correspond with time is recorded. With this software, the data obtained can be used for other purposes and can be exported to various file formats.

The cut rock was collected by using brush and scoop. The collection finer particle size fractions was carried out with an industrial vacuum cleaner where a cotton cloth was interposed as a filter.

4.6 Methods of Cutting test, Parameters, Properties of Rock.

To obtain an accurate result and clearer picture of investigated components (cutting force, side force, normal force) 30 cuts were performed in each layer. However, the fist cut was not taken into account during the measurements, because it was a blocked cut. After each layer the surface was leveled for comparison with the results of the first and subsequent layers. However, this is not applicable in practice.

On the other hand there was a problem with leveling process. This process took a lot of time that has not been allotted to plan. Therefore, during the cutting

process only one block (half radiated) was cut . Further all the results are shown only for this block.

Cutting Depth and Spacing

According to the literature review, [19] [20] [23] and limitations of large scale cutting rig in order to obtain the result from cutting test the following parameters of cutting depth and spacing were chosen:
- Depth – 4mm
- Spacing – 8 mm.

Cutting Length

The 390mm was selected to perform cutting test. To perform the test, there was no necessity in cutting the block through the whole length, because large pieces could fall off along the perimeter of the block. For this purpose safety zone of 120mm on each side was chosen. This zone also makes it easier to collect cut-out rocks for execution grain size test.

Cutting Speed

The cutting speed was set at 0,1m/s. This is a relatively slow speed for the cutting test to be chosen considering vibration machines for more accurate results. Another reason for the choice of low speed is particle size distribution. Small speed does not make greater distribution of rocks and has no influence on cutting force. However, cutting speed is related to the wear of pick.

Rake and Clearance Angles

The clearance angle should be from 0^0 till 10^0 , according to the literature review. In this range the cutting force is optimal and has small effect of wear to cutting tool. It was decided to take a clearance angle - 7,50. Based on the previous research [29] and with the same consideration a rake angle – $7,5^0$ was chosen. The value from 0^0 – 7,5 shows optimal cutting force.

Cutting Tool

In this study the point-attack pick was used. The bit body is made of tempered steel; the cutting tip is from a tungsten carbide alloy (fig. 4-12). To acquire accuracy of wear for each block a separate pick has been used. On the other hand, after each 3 cuts the pick had been rotated by 45^0 to get the uniform wear. The detailed sketch of pick can be found in Annex 5.
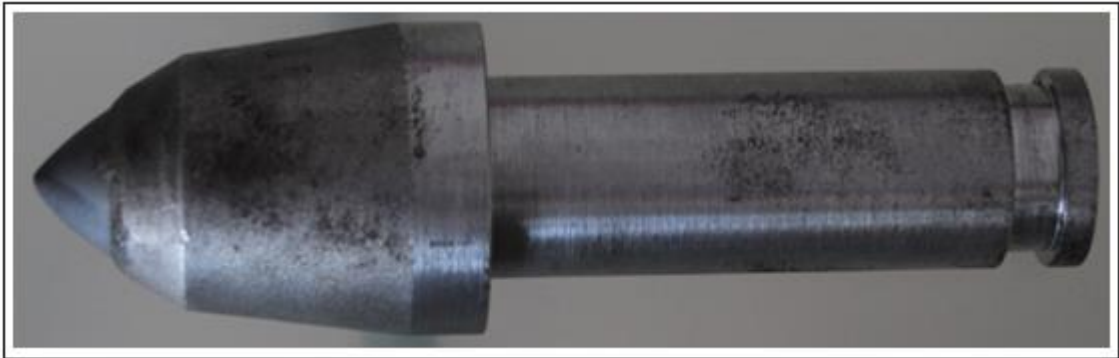
Figure 4 - 12: Point-attack pick for cutting test

The purpose of this study is to investigate the cutting resistance to hard rock. As a hard rock the three blocks of granite was selected and provided by Montanuniversität (Fig.4-13).
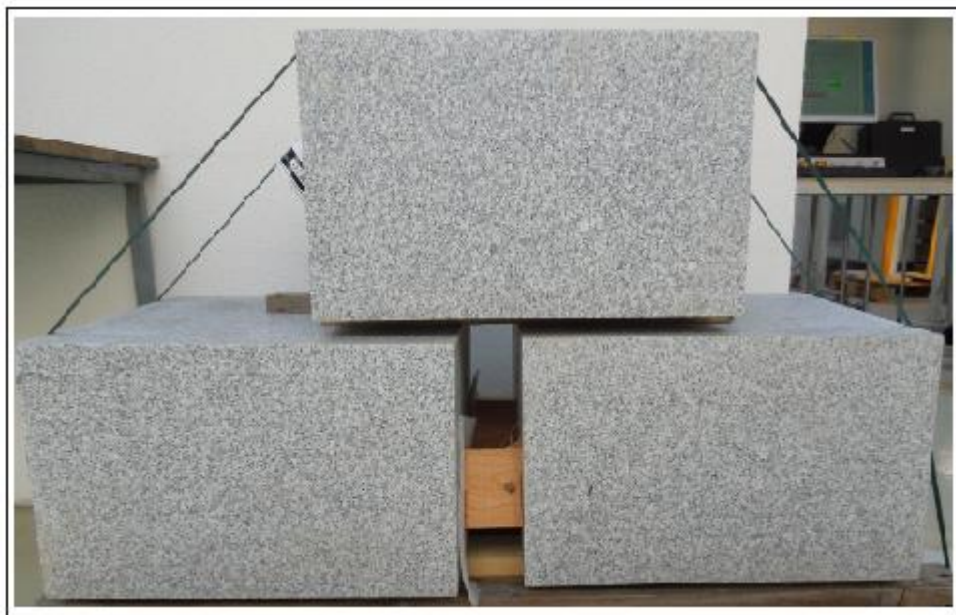
Figure 4 - 13: Granite blocks for microwave and cutting test

Each block has size 500x500X300 mm (length, width, height) respectively. The blocks were tested for chemical composition by Baustoffprüfstelle Wismar GmbH. The blocks have granular texture with some xenomorphic crystals. The main constituents are quartz, feldspar, plagioklas, biotit, muskovit and chlorit as well as additional minerals such as apatite, epidote, sphene and xenotime. The compressive strength is 202.7 MPa. Additional properties of blocks are in Annex 3.

Infrared Gun

This device was used to measure the temperature of the samples before and after the radiation (Fig. 4 -14). Infrared gun has ability to measure the minimum, maximum and average temperature emitted from the sample. All materials have different values infrared emissivity. Emissivity of material is efficiency in emitting energy from surface. This energy indicates the temperature from the object. [30]

The device was set to measure an average temperature of the surface before and after microwave irradiation.

Figure 4 - 14: High performance infrared gun

Grain Size Distribution

Particle size distribution is rocks quantitative content in the rocks of particles of various sizes. In this research a sieve analysis was used. The selected screens have the following size: 16mm, 12,5mm 8mm, 4mm, 2mm, 1mm, 0,5mm, 0,25mm.The sieves were disposed before sieving in the way that the top sieve was with the largest mesh sizes (in this case 16mm). Prior to the screening, the samples were weighed. The sum of all mass fractions after screening should not be different from the original sample weight by more than 2%. The equipment for the sieve analysis of rocks is shown in figure 4 – 15.

Figure 4 - 15: Equipment for sieve analysis

To carry out the sieve analysis was used the fallowing parameters of sieve machine:

- Time of each test – 10 min;
- Interval – 10 sec;
- Amplitude – 0,75.

In order to evaluate the quantitative composition of rock was calculated rock percentage of each layer radiated and not radiated sides. The result describes average rock percentage for radiated and not radiated side.

Estimation of Specific Energy after Cutting Test

To determine the specific energy SE for breackage rock after cutting test the formula (3-9) was aplied. The cutting force F_{smean} – will be obtained in **Chapter 5.4.** The cutting length was determined before implementation of the test.

The data for calculation of the volume of cut-out rock was obtained from laser scan. Scanning was performed after each cut layer. The raw data was stored in ASCII format, which has three dimensional coordinates (x,y,z) and then could be used for processing.

To calculate the volume the Surfer 12 sofware was used. Kriging method was applied to create a map. This method is more convinient and effective, because it allows to compensate clustered data by giving less weight to cluster. Fig.5-6 presents the view of one of the layer after cutting test.
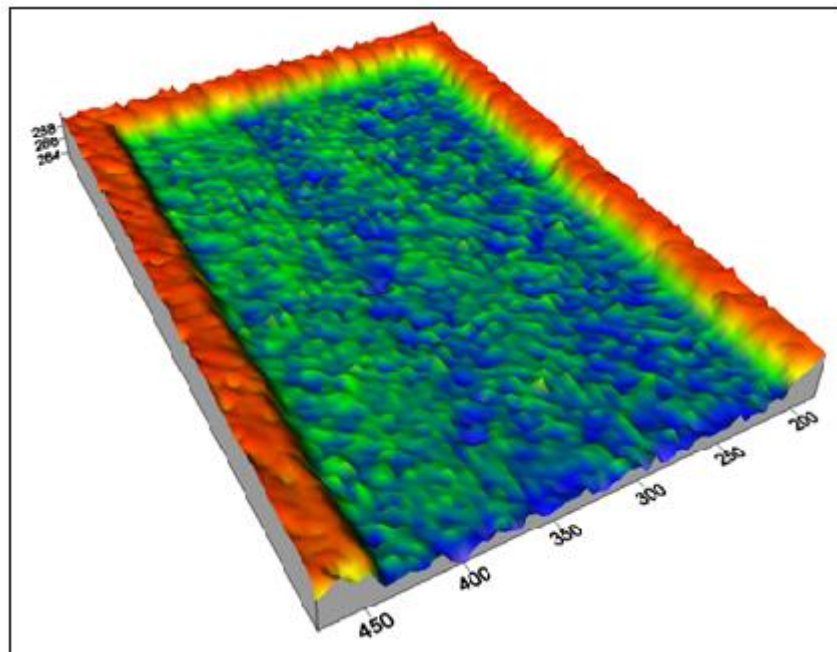
Figure 4 - 16: Surface a block after cut layer

4.7 Error Analyses

4.7.1 Volume of Cut-out Rock

To calculate a volume of cut-out rock raw data was used in software Minesight to remove unnecessary points. These points have appeared when laser couldn't be reflected from surface in a proper way or when the lighting in the laboratory was too much. Minesight allows to manage this point manually without affecting the rest of the points, as can be seen from figure 4 -17.
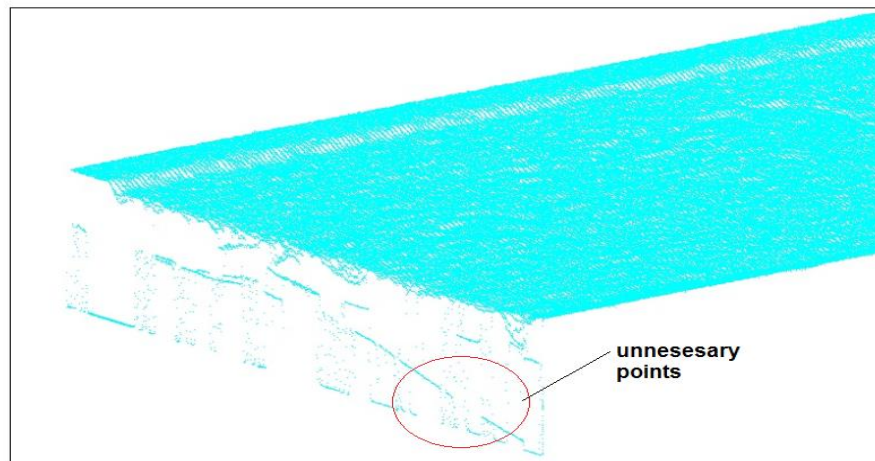
Figure 4 - 17: Model for calculation a volume in Minesight

4.7.2 Components of Cutting Force

While the cutting test was performed, sometimes a problem with sensor responsible to measure a side force appeared. Finally, the result of side force was wrong, that makes it impossible to calculate a total force. In this case the results were excluded.

4.8 Evaluation of the Data

To process the experiments, statistical analysis was applied. To determine the average value the following formula was used:

$$x = \frac{1}{n}\sum_{i=1}^{n} x\,i = \frac{1}{n}(x1 + \cdots + xn). \qquad 4-1$$

This formula (5-1) was applied for calculation of resultant force:

- Fcmean – $F_{cuttingmean}$;
- Fsmean - $F_{sidemean}$;
- Fpmean – $F_{presuremean}$.

Since the third block was radiated halway, there was a need to divide the block into 2 parts during the calculation average cutting force, side force and normal force. First part of the block is the area where there was radiated block and the second area is an untreated part. The schematic separation of the block is shown in Fig. 4 -8.
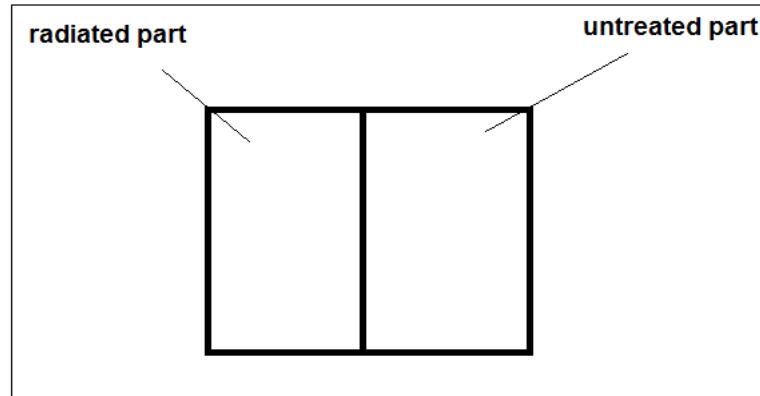
Figure 4 - 18: Top view of the half treated block

The measurements of mean cutting force, side force and normal force and resulting force are shown in Annex 4. Annex 4 presents every single cut of each layer of the half treated block.

Also the standard error or the error of the mean was determined through the following formula:

$$m = \frac{g}{\sqrt{n-1}} \; (if \; n < 30) \qquad 4-2$$

$$m = \frac{g}{\sqrt{n}} \; (if \, n \geq 30) \qquad 4-3$$

Where g - standard deviation; n - sample size.

With a standard error given by 95 % confidence interval equal to ± 2 m, it indicates the range zones in which the probability p = 0.95 gets the average of the general totality MX (in this case mean of resulting force). Since the cutting force Fc has essential meaning in this study the variation coefficient was determined via formula 4-4.

$$V = \frac{\sigma}{\vec{x}} * 100\% \qquad (4-4)$$

41

Where V – variation coefficient, σ – mean-square deviation, $\vec{x}$ – average mean of cutting force.

Testing the Assumption of Normal **Distribution of Cutting Force**

In this work Pearson's chi-squared test ($\chi 2$) was chosen to test the hypothesis according to the empirical distribution of the intended theoretical distribution F (x) at a sample size n = 29 (n - number of cuts in a single layer). The test results are shown in Table. 4-1.

Table 4 - 1: Average cutting for

#	Fmean(kN)
1	7,41
2	6,92
3	7,47
4	7,50
5	6,92
6	6,85
7	7,08
8	6,53
9	6,65
10	6,27
11	6,24
12	7,70
13	7,53
14	7,88
15	7,98
16	7,83
17	6,86
18	6,93
19	6,59
20	6,87
21	6,98
22	6,84
23	7,31
24	7,24
25	7,23
26	8,57
27	8,42
28	9,50
29	9,27

Using Pearson's chi-squared in orderto test the hypothesis that the distribution of the random variables Fmean does not contradict the normal law on the confidence level α = 0,05. The amplitude excursion **R$_{Fmean}$=F$_{mean(max)}$-F$_{mean(min)}$=3,26** kN. Determine the number of classes "N" for which to split the empirical distribution histogram. To determine the number of classes the following formula is used. [31]

$$N = 1 + 3.32 \lg(n) = 1 + 3.32 \lg(29) = 5,86 \qquad 4-5$$

In this case was taken – 5. For the 95% confidence level and degrees of freedom $f = N - 3 = 2$ critical Pearson equal χ_{cr} =6.25 [32]. To compute the actual frequency and distribution of the theoretical random variable was created a Tables 4-2; 4-3; 4-4.

Table 4 - 2: Statistical Analysis

Number of interval i	class boyundary		Variant	freaquensy		
	x_i	x_{i+1}	$x_i^* = \dfrac{x_i + x_{i+1}}{2}$	n_i	$x_i - \bar{x}$	$x_{i+1} - \bar{x}$
1	6,24	6,89	6,57	9	–	0,47
2	6,89	7,54	7,22	12	-0,47	0,18
3	7,54	8,19	7,87	4	0,18	0,83
4	8,19	8,85	8,52	2	0,83	1,49
5	8,85	9,50	9,18	1	1,49	–
Sum				28		

Table 4 - 3: Statistical Analysis

Number of interval i	Normalized interval limits		The values of the Laplace function		Interval probabilities	theoretical frequency
	$z_i = \dfrac{x_i - \bar{x}}{\sigma}$	$z_{i+1} = \dfrac{x_{i+1} - \bar{x}}{\sigma}$	$\Phi(z_i)$	$\Phi(z_{i+1})$	$P_i = \Phi(z_{i+1}) - \Phi(z_i)$	$n_i' = n \cdot P_i$
1	$-\infty$	-0,579	-0,5	-0,22	0,28	8,294
2	-0,579	0,228	-0,22	0,09	0,31	8,874
3	0,228	1,039	0,09	0,351	0,261	7,424
4	1,039	1,853	0,351	0,468	0,117	3,451
5	1,853	∞	0,468	0,5	0,032	0,841
Sum					1	29

Table 4 - 4: Statistical Analysis

Number of interval i	freaquensys		$(n_i - n_i')^2$	$\dfrac{(n_i - n_i')^2}{n_i'}$	n_i^2	$\dfrac{n_i^2}{n_i'}$
	n_i	n_i'				
1	9	8,294	0,498	0,172	81	10,3
2	12	8,874	9,771	1,270	144	16,58
3	4	7,424	11,723	1,497	16	2,18
4	2	3,451	2,105	0,572	4	1,17
5	1	0,841	0,025	0,006	1	1,07
Sum		29		$\chi^2 = 3,51$		

The Laplace function was determined via formula.

$$\phi(z_i) = \frac{1}{\sqrt{2\pi}} \int\limits_{0}^{z_i} e^{-\frac{z^2}{2}} dz \qquad\qquad 5-6$$

The ordinates represent the number of measurements falling on each interval. The distribution of the random variables is shown as a histogram and the theoretical distribution - as polygon frequencies.
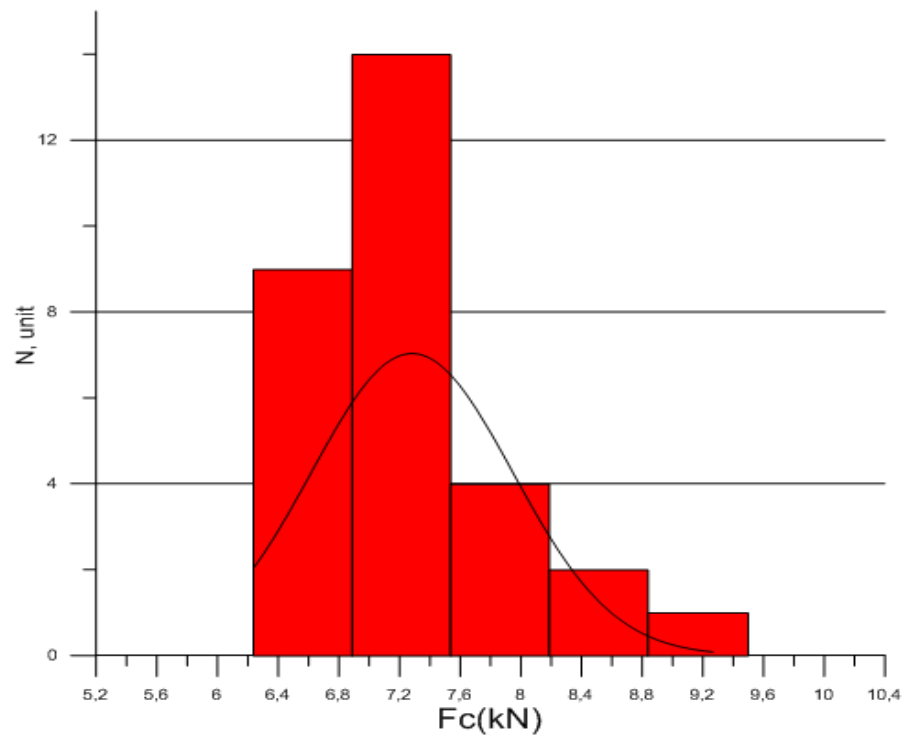
Bar chart 4 - 1: The histogram of distribution of cutting force (normal distribution law)

CHAPTER FIVE

5.1. Microwave Test

Experiments were performed with continuous power of 25 Kw and radiation time 30 and 45 sec. Initial temperature of samples was 22^0C. The temperature of samples increased after 30sec heating up to 300^0C and after 45 sec up to 500^0C. After heating the sample, the radial cracks were formed in a network of cracks. The size of the cracks varies from 5 cm to 15 cm (Fig. 5-1).

Figure 5 - 1: Sample with 45 sec treatment time

Also, it can be observed that cracks size increase with the increasing emission time. In the Hartleb study [10], the formation of cracks is described that are closely related to the grain boundaries in the rock. In particular case the cracks extend along the grain boundaries. During the experiment after 45 seconds arcing effect was observed, afterwards the system automatically turns off. Another phenomenon was observed after radiation of 45 seconds. At the center of the spot pattern began to melt, forming magma (Fig. 5-2).
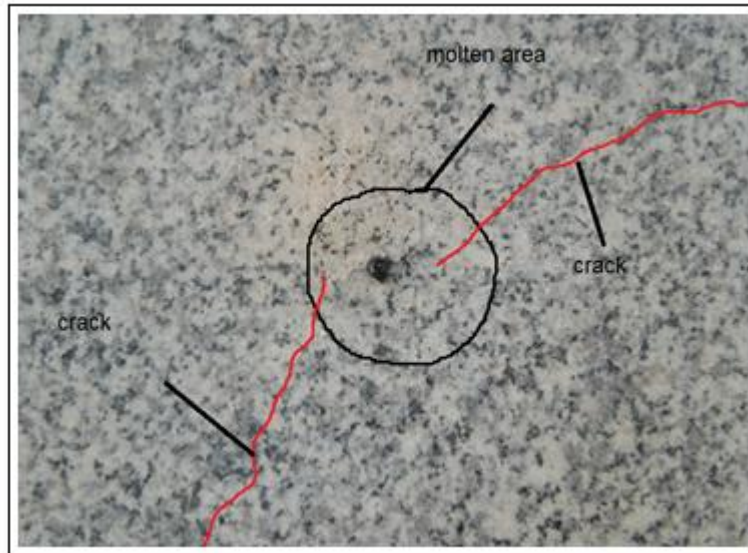
Figure 5 - 2: Molten area with cracks after 45 sec irradiation

Table 5 - 1: Overview of microwave test

Overview of microwave test					
#	output power Kw	Temperature °C	time sec	spacing between spots (cm)	effects	Input energy (Kwt*h)
1 block	25	290,42	30	10	radial cracks	111,85
2 block	25	404,84	45	10	arcs, spalation, radial crakcks, molten of grains	208,36
3 block	25	275,53	30	7,5	radial cracks	77,58

The total input energy from microwave test was calculated via formula (5 -2). The result is shown in chart 5-1.
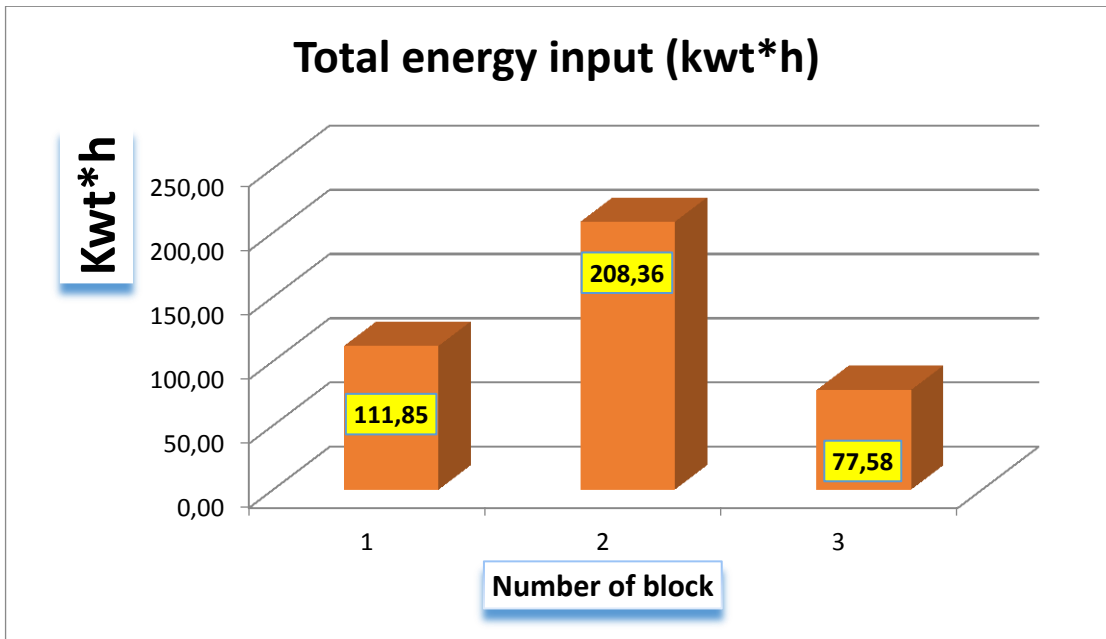
Bar chart 5 - 1: Total input energy of block

5.2. Cutting Test

5.2.1. Cutting Force

As a result of the experiment the following relationship was established: cutting force increases with next subsequent layers for both sides of block. This relation is shown in Chart 5 - 2. The increasing of the cutting force is due to the wear of pick. The wearing of pick leads to a change in its geometrical parameters which form additional cutting force.
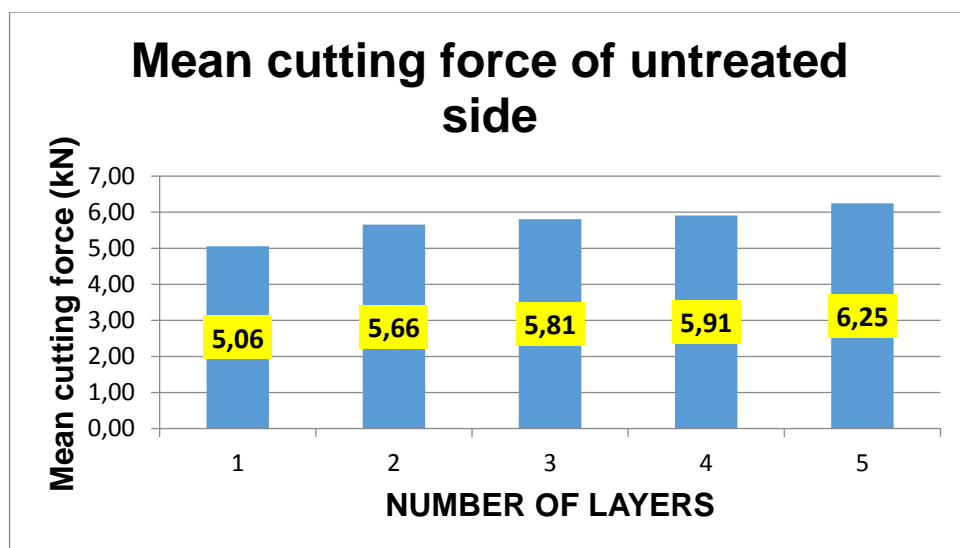
Taking into account that in calculation of specific energy is afected, only average cutting force was calculated the difference of cutting force between treated and untreated part. The result shows that average difference varies from 7% to 11%.
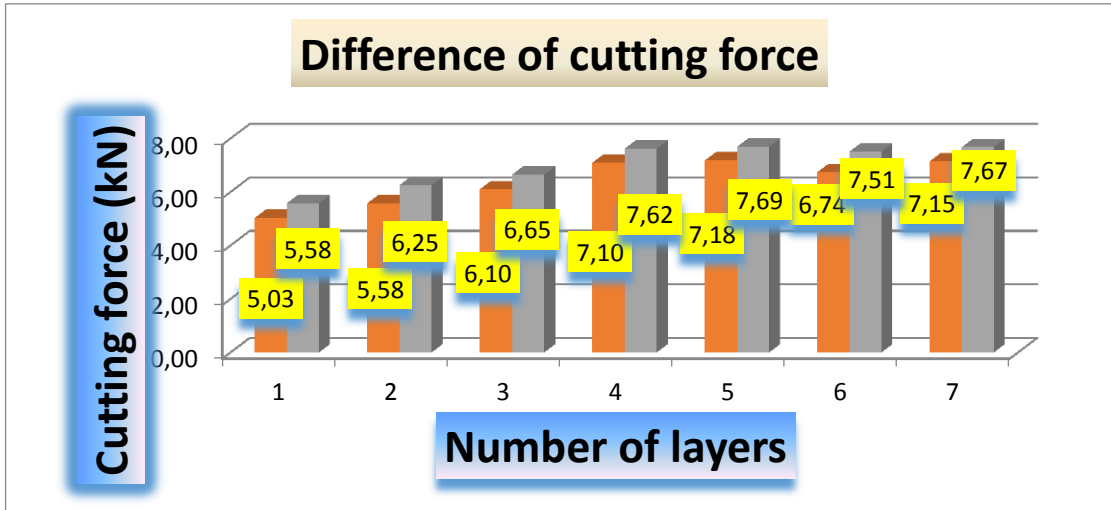
Bar chart 5 - 3: Difference of cutting force between treated and untreated part

Difference cutting force (Fc) between fully untreated and half radiated side was determined. The cutting force of fully untreated block is smaller than half-treated although the parameter of test did not change. There is a presumption that block is not homogeneous for 100% from both sides. The average difference between fully untreated and half treated is 1,5 kN.
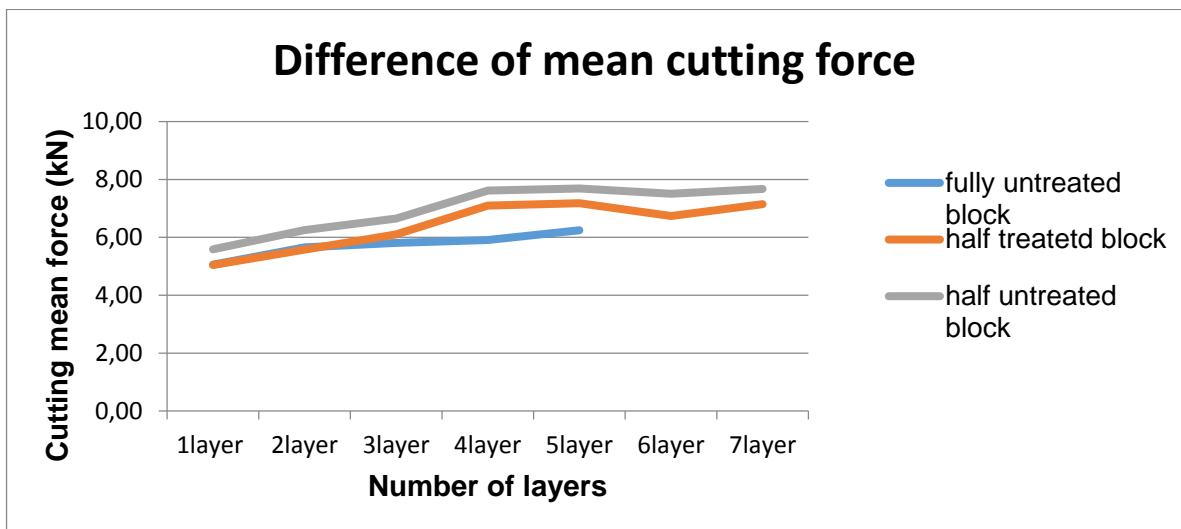
Bar chart 5 - 3: Mean cutting force fully untreated and half-treated block.

The statistical analysis was applied to check the cutting force Fc. Cutting force was checked with 95% confidence limit and obeyed the normal distribution law, except for the last two layers. The variation coefficient presents a degree of homogeneity cutting force. The data is shown in Table 5-2.

Table 5 - 2: Variation coefficient for cutting force in each layer

Number of layer	half treated	half untreated	fully untreated
1	7%	6%	8%
2	7%	9%	8%
3	10%	11%	8%
4	12%	12%	7%
5	13%	14%	7%
6	10%	12%	
7	15%	14%	

The variation coefficient varies from 7% to 15% for half radiated block,

5.2.2 Side Force

The side force (Fs) has the same relationship as the cutting force (Fc). Although there is a difference between curves in Chart 5 – 4.The side force is completely smoothed over half radiated side. The uneven force was caused due to two reasons. One is because the block was radiated unevenly (the radiated spots arranged chess-board fashion), the second from the inaccurate sensor readings.
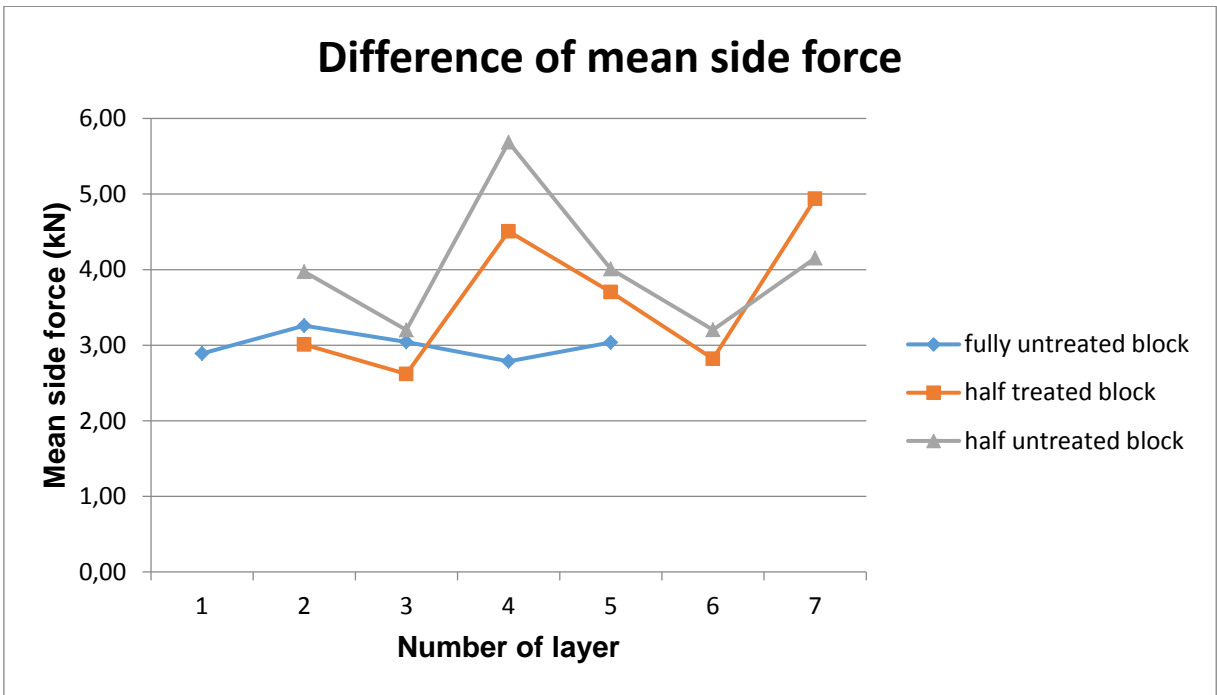
Bar chart 5 - 4: Mean side force Fs

5.2.3 Normal Force

The normal force (Fn) is one of the most important components which has influence on wear rate of cutting tool. Similar to the cutting force, normal force mostly depends on the parameters as cutting force but the value exceeds by a couple times in this cutting configuration. The half untreated side has the highest value and increases with next subsequent layer and various from 10 kN to 22kN. Treated part has the value ranging from 9kN to19 kN. Nevertheless, the result that was obtained from fully untreated side was not comparable, because was assumed that the block was non-uniform from both sides. More detailed results are shown in Bar chart 5 -5.
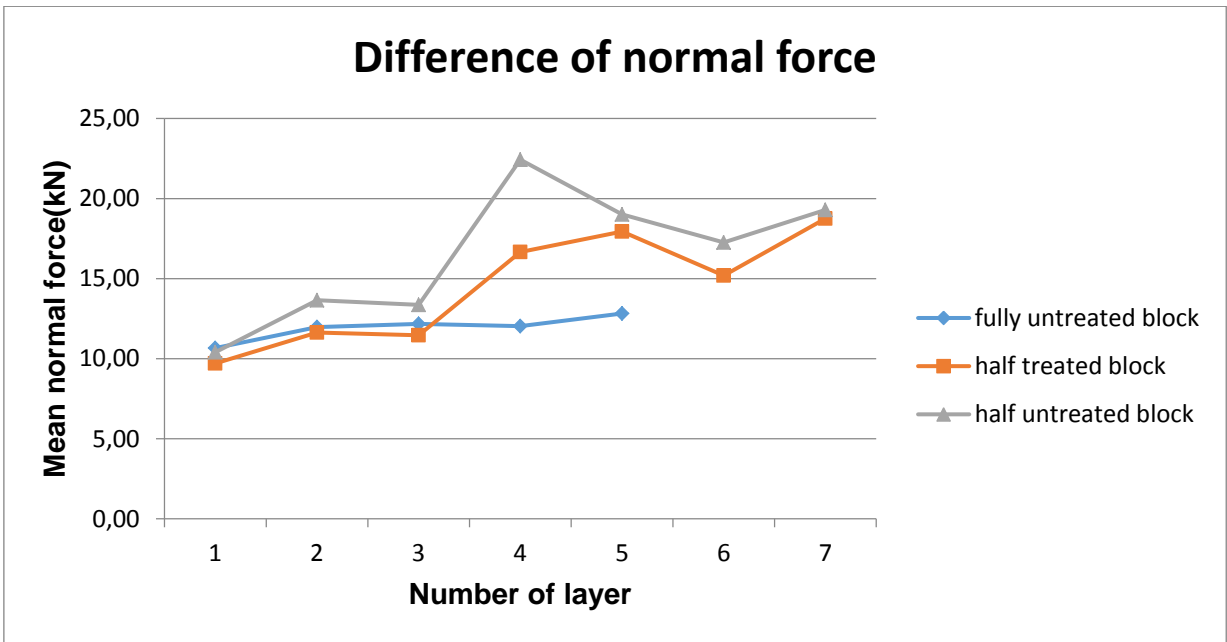
Bar chart 5 - 5: Mean normal force Fn

5.2.4 Specific Energy Consumption

Mainly, specific energy depends on cutting force (Fc). As seen from Curve 5 -5, specific energy increases with cutting force. The range varies from 3kWt*h/m^3 to 4,7kWt*h/m^3 for each cut layer, depending on treated or untreated cutting force. The total specific energy applied to half treated shown in Chart 5 – 7.
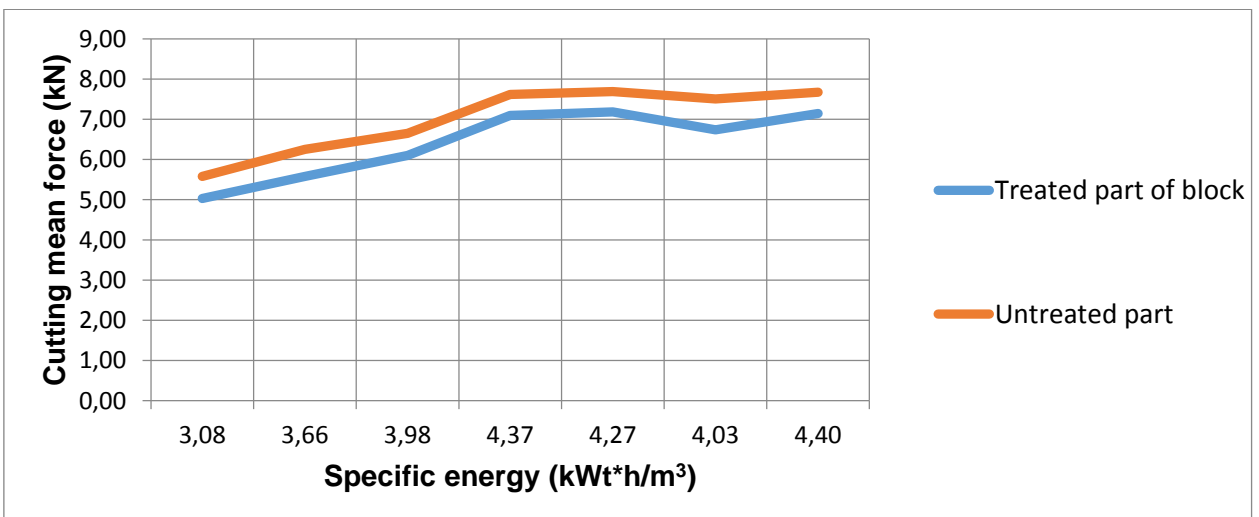
Chart 5 - 6: Ratio cutting force to specific energy
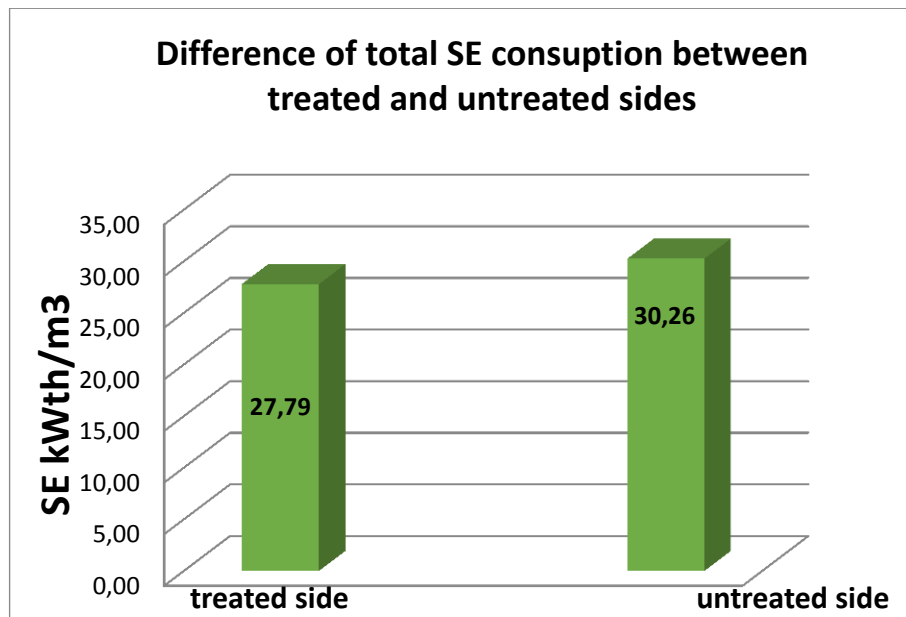
Bar chart 5 - 7: Specific energy consumption

As seen from Chart 5 – 7, in order to cut 7 layers with depth of 4 mm and spacing 8 mm 27,79 kwth/m^3 for radiated side and 30,26 kwth/m^3 for untreated side was used.

5.3 Wear Rate

To calculate a wear rate formula 3 -10 was used. The overview of results is shown in Table 5 -2.

Table 5 - 3: Data of wear consumption

# of pick	Mass before test (g)	Mass after test (g)	Difference (g)	Total cutting length m	Consumption (g/m)
1 pick	609,032	607,979	1,053	1,95	0,54
2 pick	607,964	606,528	1,436	2,73	0,53

Results show that wear rate is the same for both sides of block. It means that resulting force $F_r=F_c+F_s+F_n$ doesn't have impact on wear of cutting tool. The curve 5 – 8 presents resulting cutting force for fully untreated and half treated sides. It should be noted that this assumption is only applicable for this case and requires further evidence, because only two picks were used, which is not enough for the result.
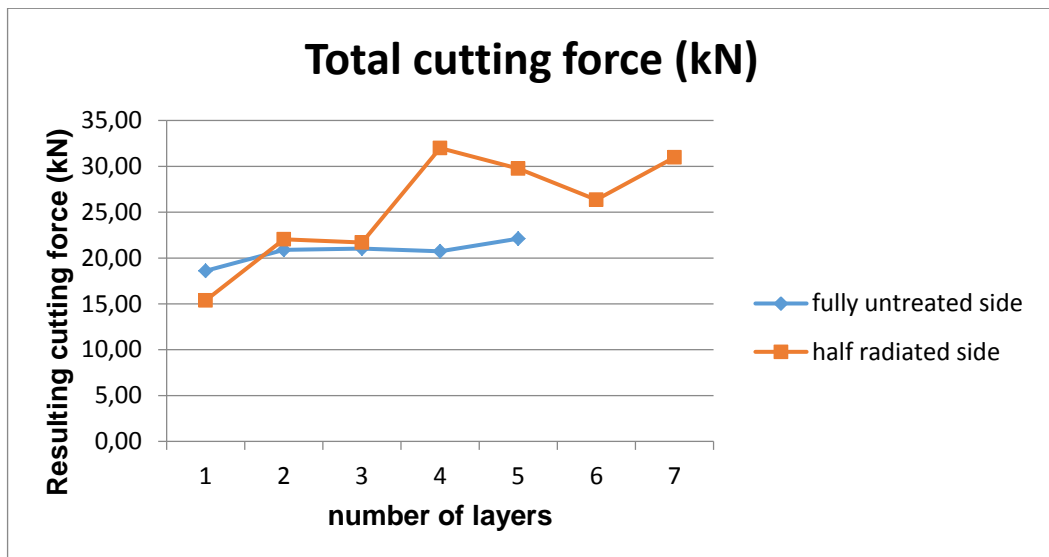
Chart 5 - 8: Resulting cutting force Fr

The total cutting force varies from 18 kN to 22 kN for fully untreated side and from 16 kN – 31 kN for half-radiated side respectively. Ratio of normal force to cutting force Fn/Fc is a significant parameter which affects wear of tool. The bar chart 5 -9 presents that this ratio is initially smaller for half-radiated block in the first three layers, but then increases. It means that wear rate depended more from ratio Fn/Fc than from resulting force.
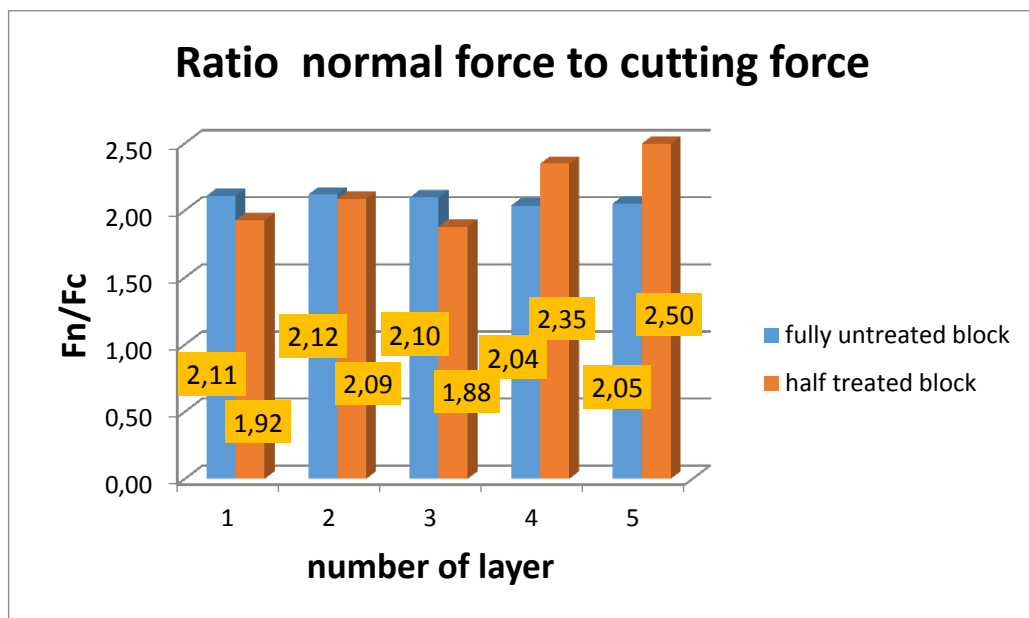
Chart 5 - 9: Ratio normal force to cutting (Fn/Fc)

5.4 Microwave assist to cutting resistance.

To illustrate how microwave treatment assists in breaking rock a model in Surface 12 (Fig. 5 -3) was created. This model shows distance between radiated spots and distribution of cutting force.
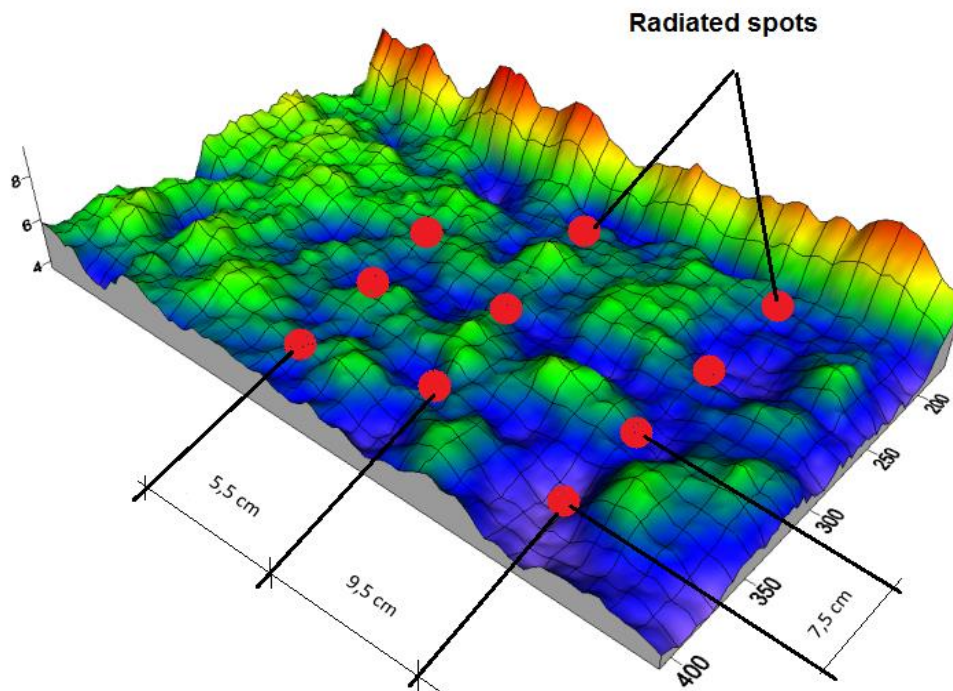
Figure 5 - 3: Distribution of cutting force on the surface half-treated block

The right side of model shows that the cutting force is bigger than the one of the others and reaches up to 9 kN. This is due to the fact that first cut is blocked and has the maximum value. Blue area is a radiated and cutting force has a minimum value (from 4kN to 5.5kN). The reduction of cutting force was facilitated by cracks that formed after microwave test. The cracks have influence on the rock properties such as hardness, strength. The cracks occur due to thermal stress. Their appearance depended on the temperature.

5.5 Seaving Analyses

The sieving analyses didn't shown significant difference between treated and not treated side of sample. The result of sieve analyses shown in table 5 – 4.

Untreated side	Sieve (mm)	weight g	%	Output in %	Treated side	mm	weight g	%	Outut %
1	16,00	0,00	0,00	100,00	1	16,00	0,00	0,00	100,00
2	12,50	0,29	0,04	99,96	2	12,50	0,41	0,05	99,95
3	8,00	9,79	1,31	98,65	3	8,00	10,70	1,30	98,65
4	4,00	135,15	18,06	80,60	4	4,00	143,25	17,44	81,21
5	2,00	141,38	18,89	61,71	5	2,00	143,31	17,44	63,77
6	1,00	84,17	11,25	50,46	6	1,00	95,03	11,57	52,20
7	0,50	89,08	11,90	38,56	7	0,50	105,68	12,86	39,34
8	0,25	93,22	12,45	26,10	8	0,25	107,20	13,05	26,29
shell	>0,25	194,87	26,04	0,06	Shell	>0,25	215,87	26,27	0,02
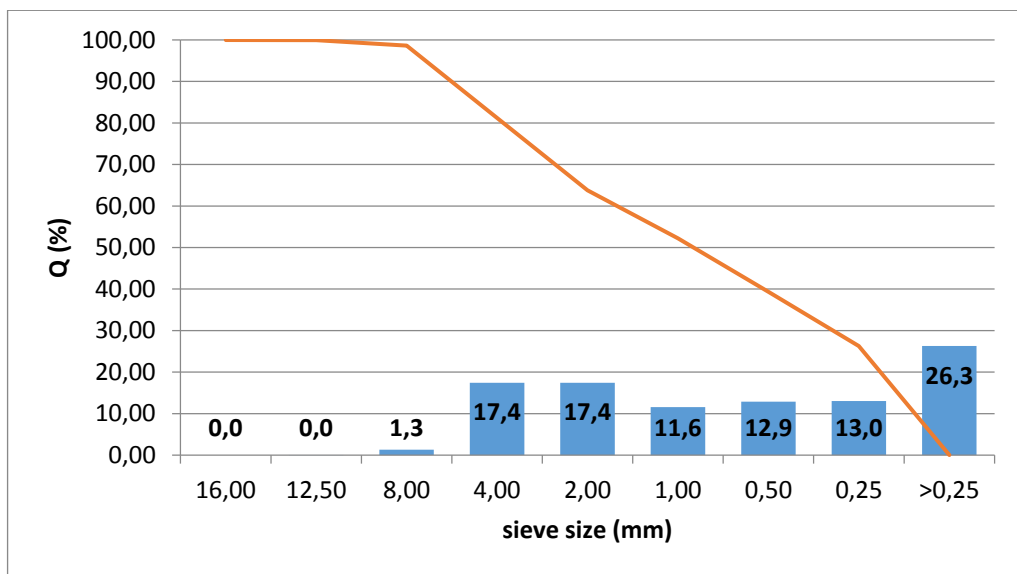
Bar chart 5 - 10: Histogram if individual fractions for untreated side
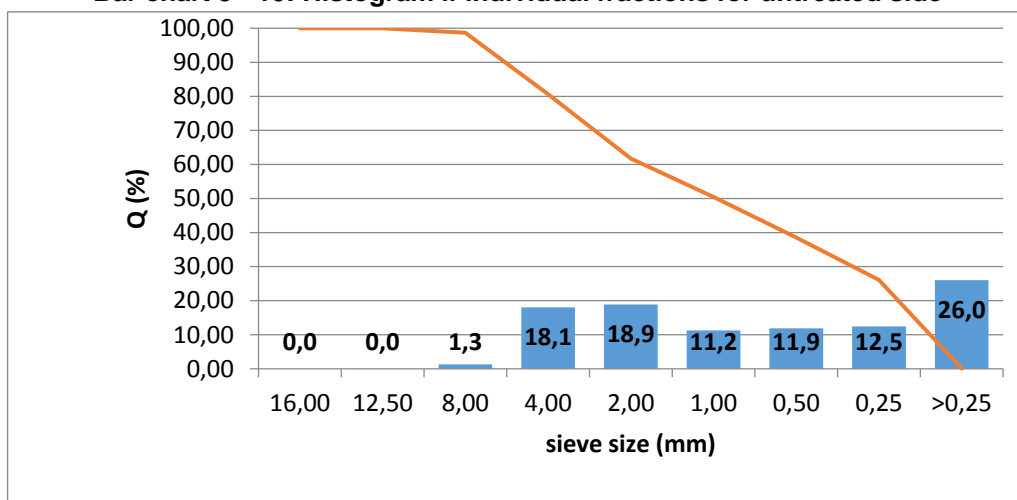
Bar chart 5 - 11: Histogram if individual fractions for treated side

The table 5 – 4 pesents average value for each sides of block. As seen from results 17% and 18,9% comprises fractions of 4mm and 2 mm respectively in both tests. The 26% comprises the fractions bellow 0,25 mm, that is not effective, because a particle size from 0,2 microns to 5 microns is most dengerous for humans and can be cause of chalicosis and silicosis. [33]

CHAPTER SIX

6.1 Conclusion

Based on this research, was obtained knowledge of influence microwave energy to cutting resistance. The granite minerals have dielectric properties, which allow the microwave energy be absorbed by rock. Absorbed energy has a thermal nature and weakens the granite. In other words, microwave energy changes the mechanical properties of rock. This effect has advantages in excavation process and can find application in mining and civil engineering. In this investigation, the cutting force has been reduced by 10% with exposure time of 30 sec for half-treated block. This means, that specific energy consumption was also reduced by 10%. However, reduction resulting force has not influence to wear rate, but this confirmation is not accurate, because the result based on wear rate of two picks. Mesh size analyses also was not shown significant difference between fully untreated and half –treated sides and present high quantities of particles below 0,25mm. Unfortunately, was not possible to determine the cutting force and specific energy consumption for another two blocks with exposure time 45 sec and 30 sec respectively due the lack of time.

6.2 Future work

According this work the future research could increase the knowledge of influence microwave to excavation rock:

1. Quantitative meaning of cracks, which had formed after microwave assist, to cutting resistance. In other words, influence cracks to strength rock.
2. In this investigation was not obtained a penetration depth of microwave. Possibilities to determine damage of volume after radiated samples. In future it has necessity to define a penetration depth for cutting test.
3. Determine optimum ratio s/d (spacing to depth) to perform cutting test for radiated samples.
4. To determine the influence microwaves to wear rate.

References

[1]   A. Olemskoy A. I, "Synergetics of condensed matter," p. 336, 2003.

[2]   V. Chanturia, "Modern problems of mineral processing in Russia," *Mining Journal,* no. 12, pp. 13-19, 2005.

[3]   H. John A. Hudson, Engineering Rock Mechanics, London, 1997.

[4]   K. P. R. J. Thuro, Roadheader excavation performance - Geological and geotechnical influences, Paris: International Society for Rock Mechanics, 1998.

[5]   F. H. a. Pejman, "ISARC," in *THE DEVELOPMENT OF MICROWAVE ASSISTED MACHINERIES TO*, Montreal, 2011.

[6]   Didenko, "Microwave Fracturing and Grinding of Solid Rocks," *Doklady Akademii Nauk,* vol. 50, no. 7, p. 349–350., 2005.

[7]   Z. M. Novik G.Y., "Management properties of rocks in the process of mining industry," *Nedra,* 1994.

[8]   W. R. Yernberg, Transactions of Society for Mining, Metallurgy, and Exploration, Society For Mining, 1990.

[9]   A. Prokopenko, "Microwave Heating for emolliating and Fracture of Rocks," in *Advances in Induction and Microwave Heating of Mineral* , Moscow, InTech, 2011, pp. 313-340 .

[10] P.Hartlieb, "Damage of basalt induced by microwave irradiation," no. 31, pp. 82-89, 2012.

[11] P. Hartlieb, "Investigations on the effects of microwaves on hard rock," Leoben, 2013.

[12] H. L. H. J. M. Muntmansky, Intriductory Mining Engineering, New Jersy: John Wiley & Sons , 2002.

[13] S. R. a. V. R., Rapid excavation and tunneling conference proceedings, Colorado: Society for Mining, Metallurgy, and Exploration (SME), 2011.

[14] S. Parker, McGraw-Hill Encyclopaedia.of Physics, vol. 2nd edition, New York: McGraw-Hill Inc., 1993.

[15] C. Rd, "Electromagnetic Radiation," The Advanced Light Source is an Office of

Science User Facility , 20 12 2008. [Online]. Available: http://www2.lbl.gov/MicroWorlds/ALSTool/EMSpec/EMSpec2.html. [Accessed 2 10 2015].

[16] S. A. Vladov M.L., Georadiolokacionie isledovaniya verhnei chasti razreza, Moskow: Moskovsky universitet im. Lomonosova, 1999.

[17] J. C. Santamarina, "Foundation Engineering: Current Principles and Practices," in *Rock excavation with microwaves*, 1989.

[18] F. K. P. M. H. K. U. R. T. Peinsitt, "Microwave heating of rocks with different water content," [Online]. Available: https://online.unileoben.ac.at/mu_online/voe_main2.getVollText?pDocumentNr=14999&pCurrPk=14652. [Accessed 10 June 2015].

[19] P. Darling, SME Hand Book, USA: Society for Mining, Metallurgy, and Exploration , 2011.

[20] B. L.I., Razrushenie gornih porod prohodcheskimi kombainami, Moscow: Nayka, 1968.

[21] Goktan, "A semi-empirical approach to cutting," *The Journal of The South African Institute of Mining and Metallurgy,* no. 105, pp. 257-264, 2005.

[22] Yasar, "Estimation Of Cutter Forces In Small Scale Rock cutting test by multivariate liner regression," *8th Asian Rock Mechanics Symposium,* pp. 1437-1446, 14-16 October 2014.

[23] H. L. Hartman, SME Mining Engineering, Colorado: Society for Mining, Metallurgy, and Exploration, Inc., 1992.

[24] S. A. Miedema, THE DELFT SAND, CLAY & ROCK CUTTING MODEL, Amsterdam: IOS Press BV, 2104.

[25] E. A. Mustafa Günay, "Investigation of the effect of rake angle on main cutting force," *International Journal of Machine Tools & Manufacture,* no. 44, p. 953–959, 2004.

[26] T. R. Onederra A., "Predicting Machine Cutting and Cutter Wear Rates for Mining," *EXPLO 95 Conference,* pp. 157-166, 9 1995.

[27] J. Dhanbad, "A Review on the Excavator Tool Bits Wear," Roorkee, 2013.

[28] Z. J.FOWELL, "DRAG TOOLS EMPLOYED ON SHEARER DRUMS AND ROADHEADERS," Ankara, 2003.

[29] B. Grafe, "Diplomaarbeit," Potential des Hinterschneidens mit Rundschaftmeißeln zur Steigerung der Schneideffizienz", Freiberg, 2014 .

[30] ScottHW, "Emissivity," 14 10 2015. [Online]. Available: https://en.wikipedia.org/wiki/Emissivity. [Accessed 9 10 2015].

[31] А. Кобзарь, Прикладная математическая статистика [для инженеров и научных работников]. – М.: ФИЗМАТЛИТ, . – 816 с., 2006.

[32] В. П. Калинина В.Н., Математическая статистика, Москва, 2002..

[33] Yshakow, "Bezopasnost gisnideyateknosti," 22 9 2000. [Online]. Available: http://www.bezo.oglib.ru/bgl/7642.html. [Accessed 17 11 2015].

[34] R. Göktan, "Effect of cutter pick rake angle on the failure pattern," *Mining Science and Technology,* no. 11, pp. 281-285, 1990.

[35] G. enciklopediya, "Granylometricheski sostav," 23 10 2013. [Online]. Available: http://www.mining-enc.ru/g/granulometricheskij-sostav/. [Accessed 17 11 2015].

List of Figures

List of Tables

List of Charts

List of Annex

1. Annex 1 Parameters of Cutting Facility
2. Annex 2 Sketch of Case for Blocks
3. Annex 3 Properties of Rock
4. Annex 4 Resulting Cutting Force
5. Annex 5 Sketch of pick
6. Annex 6 Calculation cutting test   on CD
7. Annex 7 Calculation microwave test   on CD
8. Annex 8 3D model of cutting force   on CD
9. Annex 9 Sieve analyses   on CD

Annex 1 Parameters of cutting facility

Parameter	
Baujahr	2008
Nennleistung	60 kW
Geschwindigkeiten in: x-Achse y-Achse z-Achse	 1.670 mm/s 7 mm/s 16 mm/s
Schnitttiefe (max.)	50 mm
Beschleunigung (max.)	10 m/s^2
zulässige Kräfte in: x-Achse y-Achse z-Achse	 50 kN 30 kN 50 kN
max. Probekörperabmessung: Länge Breite Höhe	 600 mm 1.000 mm 500 mm
Probengewicht (max.)	1300 kg

Annex 2 Sketch of case for blocks

Baustoffprüfstelle Wismar GmbH

Anerkannt als Prüf-, Überwachungs- und Zertifizierungsstelle

Lübsche Straße 109, 23966 Wismar; Tel.(ISDN): 03841/ 76 23 06, 7 55 48; Fax: 03841/ 76 30 78

DAP-PL-3497.00

Kurzfassung zum Prüfbericht-Nr : 2949/03 vom 05.03.2004

Auftraggeber:	Poschacher Natursteinwerk
	GmbH & Co. KG
	Poschacherstraße 7
	A - 4222 St. Georgen an der Gusen
Auftragsgegenstand:	Prüfung von Naturstein
Handelsbezeichnung:	Neuhauser Granit
Herkunft/Abbauort:	Neuhaus-Plöcking, A-4113 St. Martin im Mühlkreis

Kennwerte	Prüf-bzw. Produktnorm	Prüfergebnis
Wasseraufnahme[1]	DIN EN 13755:2002-02	0,2 M.-%
Rohdichte[1]	DIN EN 1936:1999-07	2670 kg/m³
Biegefestigkeit[1]	DIN EN 12372:1999-06	19,1 MPa
Druckfestigkeit[1]	DIN EN 1926:1999-05	202,7 MPa
Frostwiderstand einschl. Überprüfung der Leistungs-merkmale Druck- und Biegefestigkeit[1]	DIN EN 12371:2002-01, DIN EN 12372:1999-06, DIN EN 1926:1999-05, DIN EN 1341:2002-04, DIN EN 1343:2002-04	F 1 (beständig)
Abriebwiderstand[1]	DIN EN 1341:2002-04 DIN EN 1342:2002-04	14,5 mm
Verschleißprüfung[1]	DIN 52108:2002-07	6,7 cm³/50cm²
Frost-Tausalz-Beständigkeit[1]	ÖNORM B 3306:2005-12, ÖNORM B 3303:2002-09	beständig
Petrographische Prüfung	DIN EN 12407:2000-08	Granodiorit

Kurzfassung zum Prüfbericht-Nr : 1597/10[2] vom 22.02.2011

Kennwerte	Prüf-bzw. Produktnorm	Prüfergebnis
Wasseraufnahme[1]	DIN EN 13755:2008-08	0,2 M.-%
Offene Porosität[1]	DIN EN 1936:2007-02	0,5 %
Rohdichte[1]	DIN EN 1936:2007-02	2650 kg/m³
Biegefestigkeit[1]	DIN EN 12372:2007-02	17,7 MPa
Druckfestigkeit[1]	DIN EN 1926:2007-03	198 MPa
Frost-Tausalz-Beständigkeit[1]	TL Pflaster-StB 06, DIN EN 1367-6:2006-08 (Entwurf)	beständig
Frost-Tausalz-Beständigkeit[1]	RVS 08.18.01 ÖNORM EN 1367-6:2008-12	beständig

[1] Mittelwert gemäß Prüfvorschrift

[2] Wiederholungsprüfungen im Rahmen der werkseigenen Produktionskontrolle

Weitere Prüfergebnisse siehe Prüfbericht-Nr.   2949/03 und 1597/10

Wismar, den 22.02.2011

Dipl.-Ing. B. Stolge
Leiterin der Prüfstelle

Annex 4 Resulting Cutting Force

Layer 1/cutting line	Cutting force (kN)		Side force (kN)		Normal force (kN)		total (kN)	
	treated part	untreated part	treated part	untreated part	treated part	untreated part	treated	untreated
1	5,06	5,34	2,75	3,16	9,11	10,23	16,93	18,72
2	5,13	5,57	3,18	3,34	9,31	11,12	17,62	20,04
3	5,14	5,49	-0,01	-0,01	9,41	9,64	14,54	15,12
4	4,69	5,59	-0,02	-0,01	8,91	10,17	13,58	15,76
5	4,90	4,90	-0,01	-0,01	9,68	9,07	14,57	13,96
6	5,59	5,31	-0,01	-0,01	9,89	9,20	15,46	14,50
7	4,92	5,85	-0,01	-0,01	9,10	10,95	14,01	16,79
8	5,17	5,97	-0,01	-0,01	9,73	11,88	14,89	17,84
9	5,59	6,33	-0,02	-0,01	10,16	11,41	15,73	17,72
10	5,20	5,50	-0,01	-0,02	9,53	10,14	14,73	15,62
11	5,15	5,70	-0,02	-0,02	9,74	10,78	14,87	16,46
12	5,14	6,22	-0,01	-0,02	9,08	11,96	14,21	18,15
13	5,38	5,82	-0,01	-0,02	10,77	11,43	16,13	17,23
14	5,43	6,09	-0,02	-0,01	10,81	12,34	16,22	18,42
15	4,56	5,45	-0,01	-0,01	8,05	10,07	12,59	15,51
16	4,54	5,24	-0,01	-0,01	9,19	10,24	13,72	15,47
17	5,27	5,48	-0,01	-0,01	9,61	10,16	14,87	15,64
18	5,61	5,23	-0,01	-0,02	11,21	9,76	16,81	14,98
19	5,06	5,23	-0,02	-0,01	10,06	10,80	15,11	16,02
20	5,22	5,72	-0,01	-0,02	9,95	12,06	15,16	17,76
21	5,36	5,32	-0,01	-0,01	10,24	10,12	15,58	15,42
22	4,59	5,43	-0,01	-0,01	8,81	10,45	13,39	15,87
23	4,42	5,95	-0,02	-0,01	9,26	10,99	13,66	16,92
24	4,93	5,57	-0,01	-0,02	10,14	11,34	15,07	16,89
25	5,05	5,79	-0,02	-0,01	10,56	12,50	15,60	18,27
26	5,03	6,11	-0,02	-0,01	10,56	12,50	15,57	18,60
27	4,17	5,12	-0,02	-0,01	7,35	9,69	11,51	14,80
28	4,59	5,29	-0,01	-0,01	8,11	9,82	12,69	15,11
29	4,94	5,17	-0,01	-0,02	9,71	10,41	14,64	15,55

Layer 2/cutting line	Cutting force (kN)		Side force (kN)		Normal force (kN)		total (kN)	
	treated part	untreated part	treated part	untreated part	treated part	untreated part	treated	untreated
1	4,90	5,41	2,34	2,68	8,72	10,12	15,95	18,20
2	5,02	5,56	2,31	2,38	9,00	10,09	16,33	18,02
3								
4								
5								
6	5,43	6,46	2,96	3,67	9,73	11,91	18,12	22,04
7	5,88	7,02	3,07	3,60	11,55	12,36	20,50	22,97
8	5,46	5,45	2,83	2,63	10,85	9,28	19,14	17,36
9	5,65	5,33	3,22	2,84	10,27	9,43	19,14	17,59
10	4,98	5,20	2,50	2,30	8,63	8,97	16,11	16,47
11	4,80	5,83	2,41	3,01	8,66	10,44	15,86	19,29
12	5,76	6,12	3,19	3,23	10,97	11,41	19,91	20,76
13	5,44	7,04	3,11	4,10	11,18	14,14	19,73	25,28
14	5,72	6,44	3,46	4,02	11,55	14,01	20,73	24,47
15	5,68	6,48	2,70	3,12	9,86	12,00	18,24	21,60
16	6,03	6,22	2,96	3,05	11,12	11,95	20,10	21,22
17	5,59	6,08	2,57	2,75	10,66	11,57	18,82	20,39
18	5,99	6,16	3,12	3,04	11,76	11,82	20,87	21,03
19	5,85	7,11	2,90	3,59	11,38	14,44	20,14	25,14
20	6,00	7,04	2,93	3,40	11,09	14,36	20,02	24,80
21	5,36	6,19	3,16	4,11	10,83	13,60	19,35	23,91
22	5,79	6,15	3,42	3,84	11,17	12,75	20,38	22,74
23	5,87	6,25	3,29	3,75	11,42	13,08	20,58	23,08
24	5,21	6,05	2,63	2,90	9,07	11,47	16,91	20,43
25	5,25	6,47	2,53	3,08	9,02	11,86	16,80	21,41
26	6,03	6,68	2,69	3,33	10,88	12,46	19,60	22,48
27	5,75	6,61	2,76	2,91	10,19	12,09	18,70	21,61
28	5,44	6,18	2,36	2,98	9,73	11,37	17,53	20,53
29	6,18	7,01	3,01	3,97	11,64	13,65	20,83	24,63

Layer 3/cutting line	Cutting force (kN)		Side force (kN)		Normal force (kN)		total (kN)	
	treated part	untreated part	treated part	untreated part	treated part	untreated part	treated	untreated
1	6,30	6,09	2,80	2,94	12,31	12,14	21,41	21,16
2	6,14	6,31	2,86	2,90	11,75	11,37	20,75	20,58
3	6,78	7,43	3,17	3,61	13,65	14,98	23,60	26,01
4	6,95	6,89	3,51	3,62	13,41	13,39	23,87	23,90
5	6,66	7,09	3,44	3,61	13,74	14,79	23,84	25,50
6	6,53	5,82	3,23	2,32	12,43	10,34	22,19	18,48
7	5,74	6,16	2,66	2,64	11,15	11,45	19,55	20,26
8	5,70	6,53	2,72	3,13	10,99	12,07	19,41	21,73
9	5,14	5,92	2,65	3,28	8,78	10,56	16,57	19,76
10	4,66	5,77	2,23	3,02	7,96	10,47	14,84	19,26
11	5,30	4,72	2,71	2,08	9,17	8,35	17,19	15,14
12	6,12	7,47	2,83	3,65	11,05	14,25	19,99	25,37
13	6,11	6,47	3,15	3,07	11,95	12,32	21,20	21,86
14	6,68	7,52	3,34	4,03	12,66	16,91	22,68	28,46
15	5,87	6,90	2,40	3,02	10,34	13,11	18,61	23,03
16	6,12	7,12	2,64	3,30	11,15	13,84	19,91	24,25
17	6,54	7,69	2,82	3,36	12,11	15,28	21,47	26,33
18	5,63	6,98	2,28	3,22	10,22	13,73	18,13	23,93
19	6,57	6,50	2,98	2,74	12,77	13,17	22,32	22,41
20	6,94	7,52	2,92	3,31	13,90	15,32	23,77	26,15
21	5,35	6,36	2,49	3,29	9,72	11,96	17,56	21,61
22	5,81	5,73	2,87	2,92	11,45	10,87	20,12	19,52
23	5,35	5,89	2,35	2,70	10,07	11,76	17,77	20,35
24							0,00	0,00
25	6,94	7,30	3,50	3,80	13,54	15,78	23,98	26,89
26	5,79	6,62	2,51	3,53	11,14	13,65	19,44	23,80
27	6,71	7,17	2,73	2,99	12,65	13,69	22,10	23,85
28	6,44	6,81	2,91	3,07	12,14	13,99	21,50	23,87
29	5,98	7,44	2,62	3,20	11,46	13,36	20,06	24,00

Layer 4/cutting line	Cutting force (kN)		Side force (kN)		Normal force (kN)		total (kN)	
	treated part	untreated part	treated part	untreated part	treated part	untreated part	treated	untreated
1	7,44	7,37	5,49	5,51	18,41674	19,75	31,35	32,63
2	7,22	6,67	4,84	4,51	16,89	16,67	28,96	27,85
3	7,20	7,74	4,24	5,18	15,74	18,94	27,18	31,86
4	7,31	7,72	5,10	5,18	17,74	18,18	30,15	31,07
5	6,33	7,55	3,80	4,78	13,60	17,20	23,72	29,53
6	6,77	6,92	4,12	3,83	14,95	15,22	25,84	25,98
7	6,88	7,29	3,88	4,07	14,85	15,30	25,60	26,66
8	6,16	6,93	3,81	4,19	12,70	13,81	22,67	24,93
9	6,40	6,91	3,78	4,33	12,72	14,53	22,90	25,77
10	5,87	6,69	3,70	4,24	12,84	15,39	22,42	26,32
11	5,92	6,58	3,62	3,78	10,92	12,14	20,46	22,50
12	7,40	7,99	4,16	4,28	15,52	16,94	27,08	29,21
13							0,00	0,00
14	6,87	8,97	2,92	4,41	13,36	17,70	23,15	31,09
15	7,82	8,15	3,57	3,97	15,42	16,81	26,81	28,93
16	7,54	8,14	3,75	3,80	15,25	15,67	26,53	27,61
17	6,67	7,06	3,37	3,34	13,56	14,19	23,60	24,59
18	6,45	7,43	3,16	4,08	12,85	15,35	22,46	26,86
19	6,47	6,71	2,87	3,26	12,43	13,88	21,77	23,85
20	6,31	7,47	3,33	3,87	12,14	14,46	21,77	25,80
21	7,12	6,83	3,98	3,45	13,58	12,98	24,68	23,26
22	7,16	6,48	3,99	3,18	13,83	12,57	24,98	22,24
23	7,09	7,54	3,19	3,62	13,39	14,91	23,66	26,08
24	6,72	7,80	3,04	3,75	13,25	16,03	23,01	27,59
25	7,35	7,11	3,49	3,71	14,66	14,57	25,49	25,39
26	7,82	9,37	3,74	4,77	15,23	19,85	26,78	33,99
27	7,92	8,96	3,04	3,75	13,25	16,03	24,21	28,75
28	9,76	9,23	5,32	4,25	20,89	19,68	35,97	33,16
29	8,82	9,72	4,51	5,69	16,66	22,43	29,99	37,84

Layer 5/cutting line	Cutting force (kN)		Side force (kN)		Normal force (kN)		total (kN)	
	treated part	untreated part	treated part	untreated part	treated part	untreated part	treated	untreated
1	6,10	8,01	3,96	5,38	14,17	19,47	24,23	32,86
2	7,73	7,38	5,61	5,40	18,68	18,62	32,02	31,40
3	7,41	7,55	4,07	3,73	16,42	16,43	27,90	27,71
4	8,46	8,12	4,53	4,28	18,33	19,42	31,31	31,81
5	7,31	7,90	3,73	4,00	16,74	18,20	27,79	30,11
6	6,60	6,85	2,42	2,81	12,47	13,46	21,50	23,12
7	5,76	6,72	2,32	2,25	11,13	12,35	19,21	21,32
8	6,48	6,70	2,57	2,47	12,47	12,33	21,52	21,50
9	6,24	6,78	2,78	3,18	11,71	13,00	20,73	22,95
10	6,49	7,39	3,34	3,84	12,92	15,07	22,75	26,30
11	6,55	7,44	3,34	4,08	13,41	15,49	23,30	27,01
12	7,50	8,29	3,51	4,05	13,97	17,30	24,99	29,64
13	6,75	7,63	3,19	3,50	13,60	15,91	23,54	27,04
14	7,20	8,36	3,34	4,26	15,02	18,71	25,55	31,33
15	7,52	8,73	3,08	3,51	14,42	16,90	25,02	29,14
16	7,45	8,99	3,09	3,94	15,58	19,06	26,12	31,99
17	7,78	8,50	3,45	3,69	15,63	18,21	26,86	30,40
18	7,91	7,93	3,68	3,68	15,99	16,10	27,58	27,72
19	7,99	8,09	3,76	3,40	16,53	17,79	28,28	29,28
20	7,24	7,59	3,56	3,35	15,45	16,24	26,25	27,19
21	6,40	6,70	3,02	3,01	12,23	12,83	21,65	22,54
22	6,78	6,68	3,19	3,17	12,75	14,60	22,72	24,45
23	7,90	7,15	3,65	3,07	15,29	13,62	26,84	23,84
24	6,48	6,36	2,78	2,28	12,29	11,70	21,55	20,34
25	5,42	6,75	1,88	2,65	9,94	12,77	17,23	22,18
26	6,30	5,53	2,28	1,83	12,29	10,74	20,87	18,09
27	9,22	9,46	4,18	4,34	18,43	19,71	31,83	33,51
28	8,53	10,93	3,36	4,88	15,87	21,93	27,76	37,73
29	8,80	8,48	3,70	4,01	17,94	19,01	30,44	31,50

Layer 6/cutting line	Cutting force (kN)		Side force (kN)		Normal force (kN)		total (kN)	
	treated part	untreated part	treated part	untreated part	treated part	untreated part	treated	untreated
1								
2	5,94	6,41	2,95	3,82	11,30	12,65	20,19	22,89
3	5,80	6,08	3,04	3,22	11,46	12,23	20,31	21,52
4	5,63	5,81	3,10	3,14	11,80	11,89	20,53	20,84
5	6,28	6,52	3,32	3,14	12,45	12,75	22,06	22,41
6	5,33	6,19	2,81	3,11	10,54	12,27	18,67	21,57
7	5,91	6,14	2,92	2,70	12,09	12,13	20,92	20,97
8	6,08	6,88	3,23	3,62	12,68	14,33	21,99	24,83
9	5,79	6,62	2,45	3,09	11,51	13,25	19,74	22,96
10	6,69	7,17	3,73	4,16	13,47	15,08	23,88	26,41
11	7,04	8,47	3,88	4,34	14,69	17,89	25,61	30,70
12	6,77	7,70	3,38	4,17	14,25	17,23	24,41	29,10
13	6,81	7,95	3,63	4,31	14,38	18,43	24,82	30,69
14	6,57	7,75	3,29	4,44	14,49	18,01	24,35	30,20
15	7,69	9,04	6,30	7,49	21,19	23,73	35,18	40,27
16	7,42	8,53	5,62	6,91	17,45	22,00	30,49	37,44
17	6,87	7,38	5,26	5,53	16,71	18,28	28,84	31,19
18	7,05	8,52	5,37	6,93	17,88	23,75	30,31	39,21
19	7,26	8,08	5,82	6,57	19,69	20,84	32,77	35,49
20	6,39	7,26	2,45	2,57	11,48	13,52	20,32	23,35
21	6,96	7,72	2,13	3,11	12,12	14,88	21,20	25,71
22	6,49	7,29	2,25	2,24	11,84	14,27	20,58	23,80
23	7,13	8,69	2,62	3,09	14,35	17,66	24,10	29,44
24	7,96	7,97	3,03	2,75	15,69	17,03	26,68	27,75
25	7,59	8,45	3,51	4,31	15,85	18,83	26,95	31,59
26	7,64	8,02	3,44	3,68	14,83	17,56	25,92	29,26
27	7,37	7,63	3,51	3,91	15,69	16,99	26,57	28,53
28	7,58	8,05	3,49	3,57	15,83	17,59	26,90	29,20
29	6,66	7,89	2,82	3,20	15,19	17,26	24,67	28,36

Layer 7/cutting line	Cutting force (kN)		Side force (kN)		Normal force (kN)		total (kN)	
	treated part	untreated part	treated part	untreated part	treated part	untreated part	treated	untreated
1	7,57	8,63	6,11	7,30	19,21	23,63	32,90	39,56
2	7,45	8,09	5,76	6,72	18,19	22,11	31,40	36,91
3	7,54	7,94	6,07	6,37	19,43	21,13	33,04	35,43
4	7,58	7,77	6,19	6,83	20,17	23,22	33,93	37,82
5	4,60	4,77	2,18	1,65	8,42	8,60	15,20	15,02
6	5,04	5,34	1,98	2,20	9,62	10,28	16,63	17,82
7	4,71	5,18	1,85	1,93	9,12	9,41	15,68	16,52
8	4,96	5,66	1,73	2,36	10,16	11,47	16,85	19,49
9	5,57	6,00	2,34	2,50	10,56	11,66	18,47	20,16
10	8,21	8,00	5,12	5,10	18,97	19,75	32,31	32,85
11	7,41	7,81	4,38	5,25	17,37	20,95	29,16	34,01
12	8,24	8,10	5,25	5,54	19,58	21,20	33,07	34,85
13	7,77	7,94	4,49	4,87	20,07	20,07	32,32	32,88
14	6,76	8,11	4,12	4,83	16,79	19,78	27,66	32,73
15	7,76	8,57	5,48	6,48	20,67	23,20	33,91	38,24
16	7,87	9,36	5,97	6,99	20,61	24,89	34,45	41,24
17	7,82	8,43	6,20	6,95	21,48	23,37	35,51	38,75
18	7,92	8,44	5,57	6,27	22,61	22,61	36,09	37,32
19	8,18	8,37	6,97	6,73	22,65	22,50	37,81	37,60
20	6,88	7,81	3,63	4,23	15,87	17,40	26,39	29,45
21	8,12	8,44	4,18	4,64	17,72	19,25	30,02	32,33
22	7,55	7,86	4,06	4,62	17,14	18,49	28,76	30,96
23	7,84	7,71	4,61	4,28	18,60	18,60	31,05	30,59
24	7,43	8,47	3,73	4,38	16,53	18,40	27,69	31,24
25	7,29	8,18	3,91	4,46	16,47	18,25	27,67	30,89
26	6,93	7,98	3,79	4,34	15,48	18,74	26,20	31,06
27	6,80	7,68	3,56	4,27	15,20	17,92	25,57	29,87
28	7,49	8,05	4,16	4,15	19,90	19,90	31,55	32,10
29	7,93	7,89	4,94	4,15	18,76	19,29	31,62	31,34

Annex 5 Sketch of pick